Robust adaptive control of current in test equipment for lithium ion battery systems

L I N U S S J Ö V A L L

Master of Science Thesis
Stockholm, Sweden 2014

Robust adaptive control of current in test equipment for lithium ion battery systems

L I N U S S J Ö V A L L

Master's Thesis in Systems Engineering (30 ECTS credits)
Master Programme in Aerospace Engineering (120 credits)
Royal Institute of Technology year 2014
Supervisor at KTH was Per Enqvist
Examiner was Per Enqvist

TRITA-MAT-E 2014:13
ISRN-KTH/MAT/E--14/13--SE

Royal Institute of Technology
School of Engineering Sciences

KTH SCI
SE-100 44 Stockholm, Sweden

URL: www.kth.se/sci

Abstract

This thesis project have the purpose of investigating possibilities for a current control with respect to cell voltages in the testing procedures of large battery systems. The main goal is to design and implement a control that is not in need of considerable tuning, but still has stability and performance during all different conditions of testing. The dynamics of the battery system is largely dependant on the temperature, but other factors such as age also affect the behaviour, and most importantly the dynamics changes for different battery systems.

Current control in a battery cell is relatively easy and with classic control theory methods one can achieve robustness with regards to stability, and this is largely used as a foundation for evaluating possibilities. To achieve good performance an adaptive control method is selected, where the changing gain of the system is one of the most important properties to determine. More specifically, a parameter based recursive least squares method is applied. Some special consideration is taken within designing the control to work in the digital networked system that constitutes the test rig with battery system, actuator and control.

Generally, the significant properties of the cells in the battery system can be determined by the adaptation, and the performance is good considering the responsiveness of the subsystems surrounding the control. However, there are parts that may still be improved within the control by considering compensation for imperfections in the network and the treatment of data in closed systems.

Sammanfattning

Detta examensarbete har som syfte att undersöka möjligheterna till reglering av ström efter börvärde på cellspänningar i testning av stora batterisystem som är ämnade att användas i tunga hybridfordon. Det huvudsakliga målet är att utveckla och implementera en regulator som inte är i behov av större parametersättning men fortfarande behåller robusthet och prestanda vid olika typer av testning. En av de största faktorerna utöver byte av batterisystem är de förändringar som sker i celler vid olika temperaturer.

Reglering av ström i battericeller är relativt enkelt och klassiska metoder för regulatordesign kan uppnå robusthet med avseende på stabilitet, och detta används till stor del för utvärdering av möjligheter till prestandaförbättring. För att uppnå snabb reglering används adaptiv reglerteknik där den varierande förstärkningen i systemet är viktigast at ta hänsyn till. Specifikt så används en parameterbaserad rekursiv metod där cellernas egenskaper bestäms under användning. Dessutom appliceras vissa kompensationer i form av tillståndsmaskiner för att få önskade egenskaper i det sammansatta systemet.

De viktiga egenskaperna i cellerna bestäms med relativt hög precition utav de adaptiva algoritmerna och prestandaförbättringen mot tidigare använd reglering är stor. Dock är den slutgiltiga regulatordesignen inte optimal och vissa förbättringar kan fortfarande göras med avseende på kompensation for brister i mätenheter och behandling av data inom de inbyggda systemen.

Acknowledgements

I would like to express my gratitude towards Jakob Öman at Scania for making this project possible and for the great guidance and feedback throughout the work. I would also like to thank Per Enqvist at KTH for guidance and feedback of the academic parts of the project and Nicklas Holmström for the great help within the testing procedures, and for the input regarding properties and dynamics of the electrochemical system that batteries consist of.

Linus Sjövall
Stockholm, February 18, 2014.

Contents

Nomenclature

$\epsilon(t)$	Prediction error of input-output model. Section 5.1.
$\phi(t)$	Vector of variables in the discrete time input-output model Section 5.1.
τ	Time constant for the time dependent (RC-) circuit in the battery cell model, Section 3.1
$\theta(t)$	Vector of parameters in the discrete time input-output model Section 5.1.
a_i	Parameters of the discrete time input-output model, related to past output. Section 4.3.
A_m	Gain margin, Section 3.1
b_i	Parameters of the discrete time input-output model, related to past input. Section 4.3.
c_{cap}	Capacitance of capacitive part in the battery cell model, Section 3.1
$F(t)$	Adaptation gain, matrix or scalar. Section 5.1.
$G_{cell}(s)$	Transfer function describing a battery cell in continuous time , Section 3.1
$G_{cell}(z)$	Transfer function describing a battery cell in discrete time , Section 3.1
h	Sample or step time in the discrete time models, Section 3.1
I_{cap}	Current through capacitive part in the battery cell model, Section 3.1
I_{set}	Setpoint for the current to the current source, ideally the same as I_{sys}, Section 2.
I_{sys}	Current through the compound battery system, Section 2.
n_A,n_B	Number of past samples the input-output model depends on. If system characterized by an irreducible discrete time transfer function n_A and n_B corresponds to the number of zeros and poles respectively. Section 4.3.
R_1	Resistance of the pure resistive part in the battery cell model, Section 3.1.

R_2 Resistance of the time dependent resistive part in the battery cell model, Section 3.1.

V_{cap} Voltage across the capacitive part in the battery cell model, Section 3.1

V_{cell} Voltage across a single cell in the battery cell model, Section 3.1

$V_{lim,max}$ Lower cell voltage limit, Section 2.

$V_{lim,max}$ Upper cell voltage limit, Section 2.

V_{max} Maximum cell voltage in the battery system, Section 2.

V_{min} Minimum cell voltage in the battery system, Section 2.

$V_{OCV}(t)$ open circuit voltage (OCV) of battery cell, may be constant or time dependant, Section 3.1

V_{sys} Voltage of the compound battery system, Section 2.

1 Introduction

1.1 Background

Within the charging and discharging of batteries and battery systems there is a number of factors to consider, both in actual usage and in the testing and development of products involving batteries. Among the most important aspects are the current and voltage limits that are to be followed to avoid damage or accelerated ageing.

In this thesis the possibilities of controlling the maximum charge- and discharge current in large hybrid electric vehicle (HEV) battery systems is investigated, where the voltage limits of the worst individual cell is setting the governing bounds. The main objective is to find a control method that, with minimal amount of active retuning, can be used on different systems under different circumstances with good performance. Important variations include different cell chemistry, system configurations, temperatures, state of charge and age of the cells. The knowledge of the dynamics and properties of the cells are limited since the controller is to be used within the early testing phase, but base properties that is present on a data sheet for a sample cell is known, such as one or a small set of typical internal resistances. Additionally, the configuration of the cells within the battery system is known.

The primary usage of the control will be in *hybrid pulse power characterization* (HPPC) tests, which consists of high current pulses of short duration at different amplitudes (the exact method is based on an existing ISO standard [12]). But there is also a need for functionality within other experiments such as lifetime testing with actual drive cycles (these test methods are also described in [12]). Common for the applicable testing is that it is specified in the form of current profiles.

Previously, a statically tuned PID based controller have been used for a specific battery system with decent performance, but more performance is desirable to avoid aborting a test as well as robustness so that one controller can be used with different battery systems.

1.2 Method

Important for the accuracy in the application is understanding of the set-up and the behaviour of the different components, not only the battery cells but also the measurement equipment, the actuator in form of a voltage or current supply and network effects. Section 2 explains the test set-up and the parts that affects the design process, followed by an explicit formulation of the system model in Section 4. This is linked to an investigation of the system response with classic control theory that is useful as a foundation for further investigation, due to the changes in system properties a method based on adaptive control is finally selected (as in Section 5).

The work is linked to simulations that largely could be based on measurement data from earlier tests. The simulation results and the results of the final implementation in the testing environment is covered in Section 6 together with evaluation of

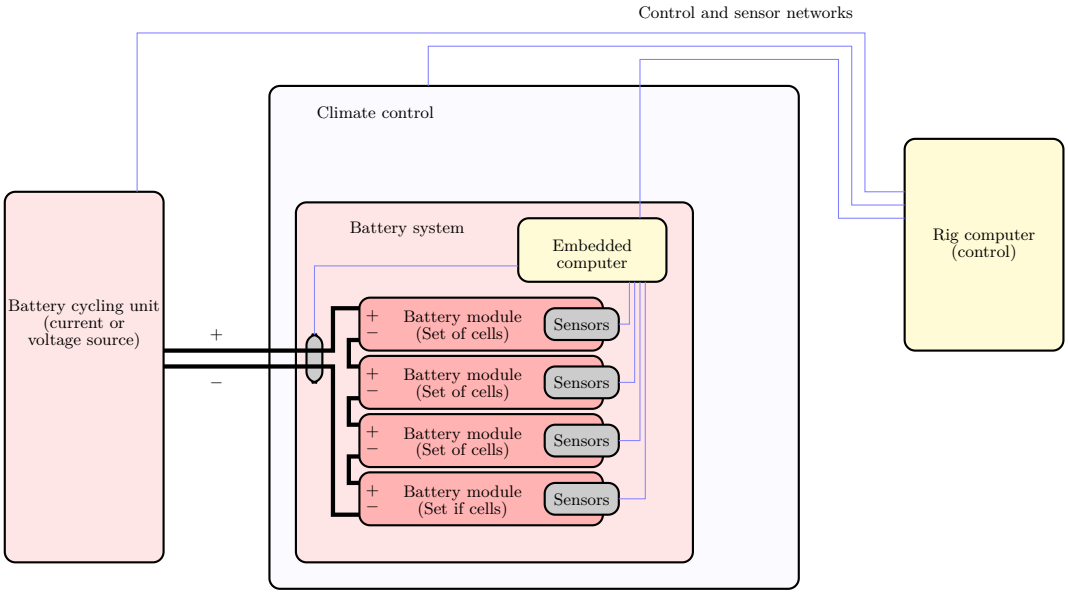

Figure 1. Overview of the test equipment set-up with battery system, actuator and control. The battery system consist of cells as well as sensors and an internal computer for sensor communication, balancing and other functions.

the results. With a goal of a control that is functional in actual usage, the methods of the thesis are tested along ordinary experiments on the battery systems.

2 Equipment and testing setup

The basic test set-up is shown in Figure 1, it consists of a battery system connected to a battery cycling unit capable of supplying a constant voltage or a constant current depending on the selected mode. In addition, a climate control equipment is used for performing tests at different temperatures.

From a control perspective the battery is to be viewed as the system to control and the cycling unit as the actuator, which may from now on be referred to as the cycling equipment, the current source or the actuator. The general control loop from a control perspective is shown in Figure 2. The different devices are connected to a rig computer via different types of control networks, mainly CAN (controller area network) buses. This computer handles the overall control of the equipment.

Battery system configurations The battery system is designed for applications within heavy hybrid electric vehicles, as an energy storage with the capacity to transfer high amounts of energy in or out of the system. To keep the current within a reasonable level the voltages are raised to high values. The battery cycling equipment is capable of magnitudes up to 900 volts, and currents up to 500 A. These large current and voltage values highlights the importance of stability

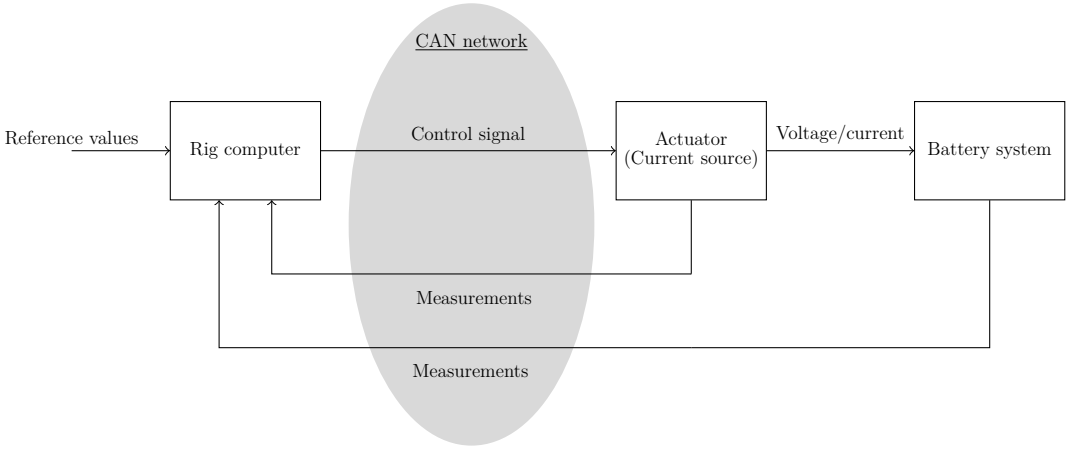

Figure 2. Overview of the control loop.

and robustness, partly because of the expensive equipment involved. The battery configuration achieves the needed specifications by using a large number of cells, in both series and parallel configurations. For practical purposes they are usually arranged in physical modules (Figure 2) that do not directly affect the electrical layout, but it is important to know that the different measurements are done with different hardware. As an example an eight cell battery system may consist of two modules in series, each consisting of four cells, two in parallel and two in series. This would yield a system with four cells in series and two in parallel. The modules are consisting of a limited number of cells both in parallel and in series as well as the sensors. The modules are then stacked to a complete system, there is still only one terminal to connect a load, a general view of the circuit is shown in Figure 3 where each rectangle corresponds to one cell. Thus, when considering the control, the system have a single input (in actual usage this is the current I_{sys} but could also be the voltage V_{sys}) and multiple outputs in the form of measurements of each cell voltage and other quantities such as temperatures at different locations. The individual cell voltages are denoted $V_i,\ i \in \begin{Bmatrix} 1 & 2 & 3 & \dots & n \end{Bmatrix}$ [1] as in Figure 3 and since all cells in parallel have the same voltage (by Kirchoff's voltage law) only the voltage differences between cells in series needs to be considered.

Each measurement is handled by the integrated logic and sent as a message over the CAN bus with a fixed interval that differs between the quantities and the different battery systems. From the previous testing it is clear that the measurements of the *individual cell* voltages V_i is subject to a larger delay than the total voltage V_{sys}. This delay is related to the different hardware involved, but as it is a closed

[1] The voltages V_i are individual cell voltages, typically in the range of $3-4$ V for lithium based cells, not to be confused with the voltage of a module, that may be in the region around $10-50$ V. In these applications there are generally hundreds of cells, arranged within tens of modules.

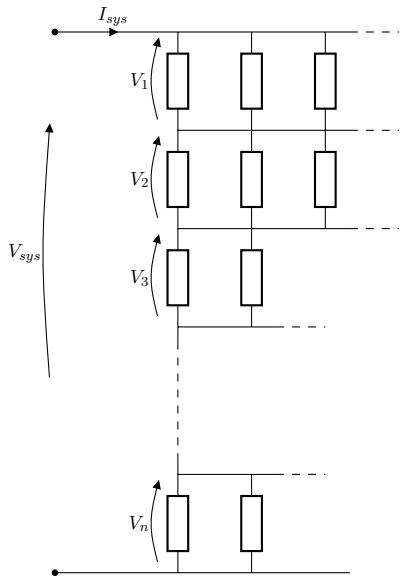

Figure 3. Overview of a general battery system cell array, the modules are not shown as they are only a physical division that does not affect the electrical layout.

system that will change it has not been investigated further. The control design is done with enough robustness to handle a large delay of individual cell voltage measurements. In practice it is reasonably clear that some type of filtering of raw data has occured, by either analog or digital circuitry.

As the worst individual cell sets the limit one mainly considers the maximum and minimum cell voltage

$$V_{max} = \max(V_1, \ldots, V_n) \quad \text{and} \quad V_{min} = \min(V_1, \ldots, V_n) \tag{1}$$

and the upper and lower voltage limits that we denote $V_{lim,max}$ and $V_{lim,min}$.

In addition to handling sensor data the embedded computer handles balancing of the cells and security functions such as contactor opening and closing.

Battery cycling equipment The actuator in the control loop is the battery cycling equipment, it is able to supply a constant voltage or a constant current (the input V_{sys} or I_{sys}) and is specified to do so with an accuracy of about 0.2%. Upper limits of currents and voltages are well above the ratings of the battery system. When considering the timing of the supplied current or voltage there is no specified performance, but the supply is surely dependent on the behaviour of the connected system. Observations of the quantities are also done by the battery cycle equipment sent with an interval of about 50 Hz.

Control computer The intelligence in the system is provided by a rig computer with LabView as the software managing the testing. It is connected to the sensor

and control networks and receives measurements from the battery systems internal sensors as well as from the external sensors in the cycling equipment. Additionally the actuators control is sent over the same network as the measurements.

The implementation of the control is performed in this already functional system. When considering the programming environment there are a set of variables easily accessible that represents all measurements, in addition to the variables that corresponds to the commands sent to the actuators. There are also basic linear algebra such as handling (multiplication) of matrices available.

This gives possibilities for easy implementation of different types of control. The limitations of the set-up are within the scheduling of the computations, there is no control over the scheduling times. Additionally, as a result of the large system with a great number of tasks, a significant amount of jitter is introduced.

3 System model

3.1 Cell model

Detailed models of the behaviour of battery cells are possible, based on either the internal physics and chemical composition of the cell or the behaviour during usage. Modelling based on physical effects in fuel cells are investigated in [5], this gives some understanding of the behaviour of cell components (anode/cathode) in a similar area. The important behaviour to model for this purpose is the response of the cell under changes in load, and more specifically, for feedback regulation purposes, it need only to be accurate within a limited frequency range (or time range) where it affects the regulators performance. This frequency range is theoretically bounded on one side by the sampling frequency and on the other side by the settling time of the control, as it will be of a feedback design. Specifically one cannot control behaviour that is faster than the sampling time, and similarly there is no need to model behaviour that is slow enough for any control system to handle. The model also needs to be general enough to work for all types of cell chemistry that might be applicable. Additionally, the different operational conditions that are applicable needs to be considered, where one of the most important factors to consider is the range of temperatures.

Equivalent circuit based ideal components

An equivalent circuit diagram is often used that may represent the system with sufficient accuracy for the application. A simple one may consist of a pure resistance in addition to a voltage source. This voltage source, describing the open circuit voltage of the cell (or $V_{OCV}(t)$) have non-linear behaviours that are not trivial to model. For investigation of these relationships, such as energy transferred and open circuit voltage, one needs to explicitly establish definitions of often used terms (such as state of charge, or SOC). For this purpose in current regulation the open circuit voltage may be viewed as constant during the short control actions, but may still

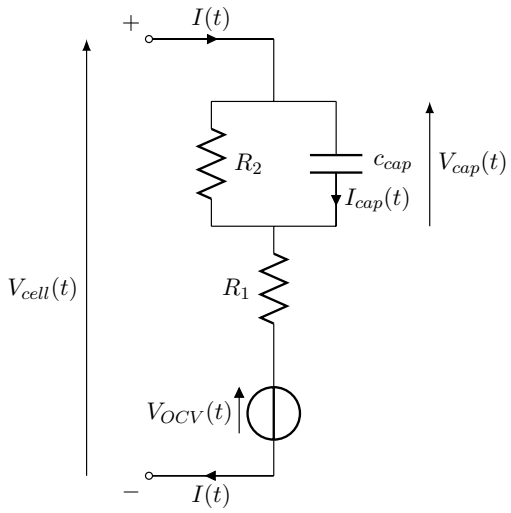

Figure 4. Cell equivalent circuit diagram.

be included in the model for specific purposes, mainly to track the change during the regulators active time.

This model can be extended with different parts and many variants exist, some are described in [2, 3] investigating lithium based cells, and the article in [4] considers nickel based cells. Common is that one or more dynamic states are introduced to the model, each of them implicitly describing either one or a group of time dependent behaviours of the cell. For investigation with focus on system control a simple model initially examined, consisting of two states where one is the open circuit voltage and the other represents a time dependent voltage. An equivalent circuit diagram as in Figure 4 describes this single cell model, that also corresponds with the model used in [1]. This model can replicate the system with good accuracy during current pulses within a limited time range, in [1] it is also evaluated with the same type of current pulses that are applicable in this thesis work.

The accuracy is naturally dependent on using correct parameters R_1, R_2 and c_{cap}. [2]

3.2 Assembled system

As said before the battery system consists of multiple cells, both in series and in parallel and there are many possibilities for a model of the complete system. A natural way is to compile a single input multiple output (SIMO) system describing each individual cell as above (Section 3.1). The system model will differ considerably if considering a voltage source as input (instead of a current source), but as only current profiles are used as input in the battery testing the model is based on this

[2]The parameter c_{cap} may be implicitly given by R_2 and the corresponding time constant $\tau = R_2 c_{cap}$ for the RC-circuit.

fact. With m cells in parallel, each one of order p, the single cell models could be combined into a SISO system of order $m \times p$. Multiple cells in series have an output voltage that is independent of each other if a current input is used and are thus easily put together to a larger SIMO system without dependencies between the states. The cell parameters would however be very similar and a model with fewer cells might produce the same accuracy, with increasing number of variables comes increased undesired computational complexity. To avoid that, another approach for the system is evaluated, namely to model just a single average cell and in addition use compensation for the extreme (maximum, and minimum) cell deviations. This model may be simplified by introducing scheduling of the deviation depending on the systems state, i.e. introduce a model for the deviation between worst and average cell at the regulation points $V_{lim,max}$ and $V_{lim,min}$ and thus avoiding some of the dynamics and nonlinearities needed for modelling of the full operational range of the cell.

In the final control a model of an average cell is used in addition to an voltage offset at the regulation point.

Closed loop Besides the cell model the sensors and actuator in the loop adds dynamics to the system that are hard to model. The accuracy regarding absolute values are high the effects of quantization are negligible. But there are substantial effects in the system in form of delay and jitter. The effect of a constant and known delay is easy to include in the model but as the behaviour of the sensors are not known between the different battery systems it becomes harder. In Figure 5 the effect of a delay of 300 ms can be seen, the result is as a phase shift which passes -180 degrees at $2\frac{1}{300\text{ms}} \approx 6.67Hz$. This represents a typical delay that is experienced with the individual cell voltage V_i of the current battery system, but with different possible systems this delay is not generally known and it is most likely a result of some type of filtering.

3.3 Parameter determination and model evaluation

Impedance. The presented model with one modelled time transient (Figure 4) can be formulated explicitly (explained in Section 4.3) and compared to the impedance of a typical cell measured by frequency sweep. In Figure 5 a comparison of the measured and modelled impedance in form of a bode plot is illustrated, with markings for the relevant frequency range. The model seen is based on a pure resistive part and a single time dependent part in form of an RC-circuit as above. As the state representing the open circuit voltage is considered constant it does not affect the impedance. The model allows for two absolute values of the gain to be specified, as well as a point in the frequency spectrum where the transient between these values appear. As we see in Figure 5 this does represent the actual cell with decent accuracy within the given range[3].

[3]note that the range in the figure is not the same as final implementation, which largely depends on sampling frequency

A general conclusion is that the absolute value of the impedance, or gain of the system, is not changing drastically within the specified frequency range (order of magnitude is around 10% change), and the improvement of accuracy possible with higher order models are limited. In addition we see the importance of the network induced delay for the model, which will be defining for the gain and phase margins (Section 4.4).

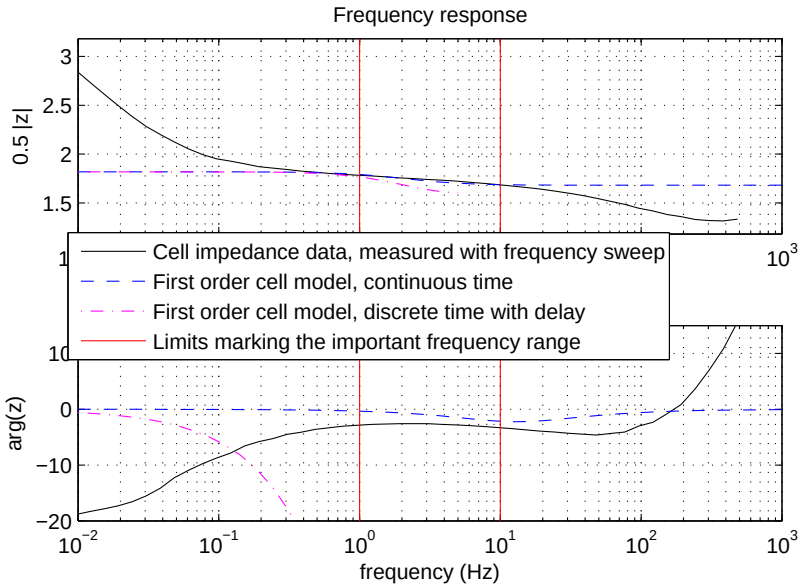

Figure 5. Frequency response of cell model compared to measurements from lithium based secondary cell, in form of a bode plot. Two models are included, one continuous and one discrete with a 10 Hz sample rate and a 300 ms delay. The Model parameters are selected to match measured gain within the given region.

Dynamics of model parameters. The model parameters are not only varying with different cells but also with different operating conditions. Temperature is one of the largest factors and a plot of the internal resistance as a function of the temperature of an example cell is shown in Figure 6. As we can see the resistive part of the cell varies with a factor of about 4 within the operational range of this particular cell, the behaviour is clearly non linear but a second order polynomial or an exponential function could be used as an approximation within given limits.

The internal resistance also varies to a lesser degree with other factors. Relations to current direction and amplitude (i.e. non-linear voltage-current relations) can be discussed as well as variations with different state of charge. However, the data from tests that have been carried out must be interpreted with care, mainly due to temperature changes during usage (testing) and internal electrochemical effects that does not have significe during regulation, but may have large effects during other parts of cell usage.

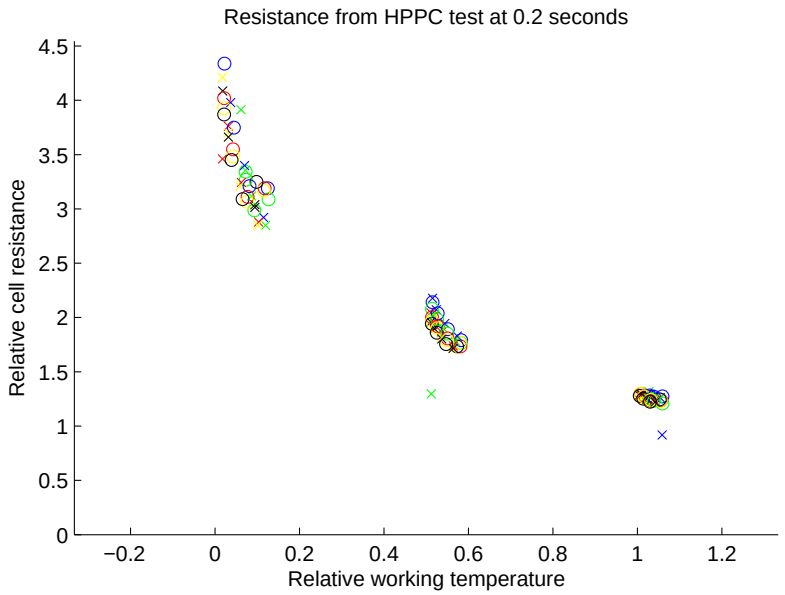

Figure 6. Values of real part of perceived resistance 0.2 s after a current step. Data is from an particular cell at different temperatures but it is not generally known. The above is normalized with a typical resistance at a typical working temperature.

Resistance viewed against state of charge can be viewed in Figure 7 at a high and a low temperature to illustrate the largest and the smallest variations. Actual state of charge is highly dependant on definition, but as seen the variations are small. Other cells in other battery systems generally have similar dependencies on temperature etc., but the absolute values and exact relation naturally differs to a large degree.

4 System control

4.1 Problem

The regulation should be designed to always keep all cell voltages within certain limits. In the application multiple such levels are specified with different actions taken when reaching each level. This is typically important when charging or discharging the battery fully, but the change in voltage related to impedance are also included within the limits. In Figure 8 some voltage regions are marked together with a typical relation to the state of charge. For this application the voltage levels are given by the manufacturer of the cells but generally they are related to destructive reactions in the cell, that may be seen as accelerated ageing and shorter lifespan.

In the application the first action is to control the current through the battery system, followed by aborting the test, and finally activating hardware security functions such as physically breaking the circuit with contactors. Most important for

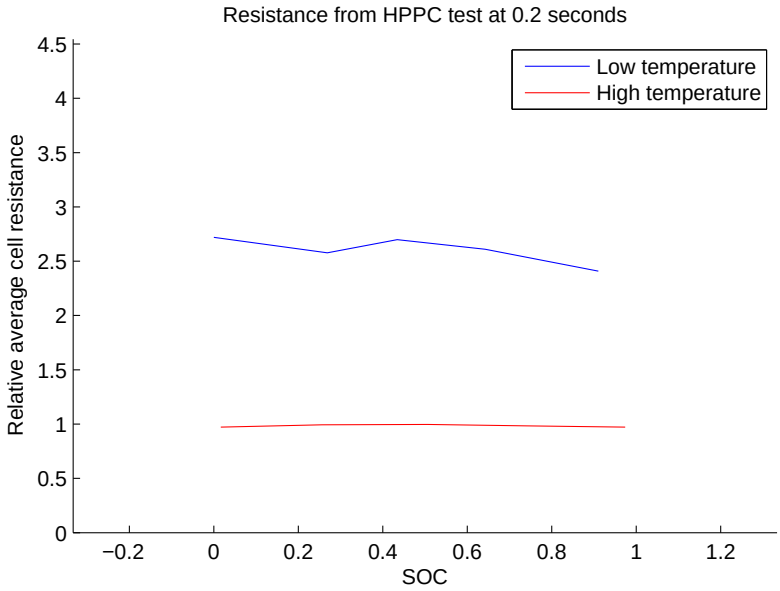

Figure 7. Some Values of real part of perceived resistance 0.2 s after a current step at different state of charge and a high and a low temperature. Axis are normalized with a typical working value of resistance and a typical working region for the used cell.

the control is to ensure stability, but high emphasis is put on performance during pulse tests which implies step response performance. Low performance in form of overshoot typically leads to an aborted test and in extreme cases one also risks to reach a voltage where the circuit is physically broken, which at large currents is destructive for the involved equipment.

When controlling the current the main system to model is naturally the battery cell and its impedance, a described above, in Section 3.1 this is formulated with differential equations. The model parameters changes considerably with different conditions and different cells, and the major problem is to achieve high performance despite this. Achieving robustness with regards to stability can easily be done with classic control theory analysis using gain and phase margins. This can be extended to cover non-linearities conservatively with, for example, the small gain theorem and/or circle criterion [6] (with certain assumptions). However, this conservative approach does have an impact on the performance. To achieve a consistently high performance an adaptive control method is the natural option while still leaving enough robustness in the system to not risk an unstable system. Many options for adaptive control exists, and the exact method to use depends largely on the conditions. In this case a parametric model is viable. With system input and output is measurable, but not internal states, a model identification adaptive control based on an input-output discrete time model is the natural choice (with several methods based on [10]). The controller itself is designed around the system model and uses

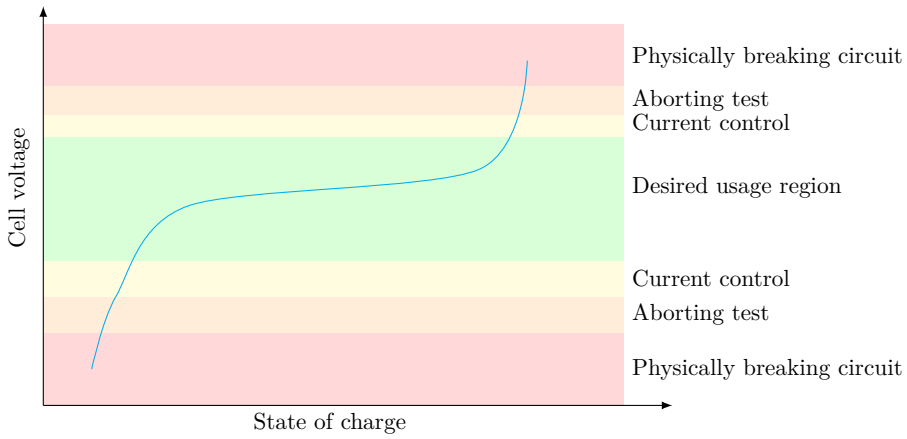

Figure 8. An illustration of how cell voltage and state of charge may be related, with desired and undesired voltage regions marked.

the adapted parameters. With a simple system as in this case it is possible to design a perfect feedback with regards to bringing the *system model* to a zero error between the output and it's setpoint.

In addition to the cell and the battery system there is other dynamics introduced, the multiple treatments of measurement data both in embedded systems as well as in the rig computer have a large effect on the system as perceived from the controllers perspective. These effects are a result of computational delay and jitter as well as dynamics and filtering in the sensors. Methods for this type of compensation have been investigated by others, but may also mitigated by assuring that the robustness of the control is good enough.

4.2 Classic methods

Previously used solution Initially, a simple statically tuned PID based controller was used in the testing purposes. This controller acted on an error signal, e, based on an actual system voltage output and a reference signal. The constant- and integrating gain is large compared to the derivative gain. From a control theory perspective it uses a conservative gain that leaves a large gain margin which makes it stable but slow to react. The control uses two states depending on which limit is relevant and effectively chooses the relevant error signal but the gain is always constant. As output it uses the maximum or minimum cell voltage (V_{max} or V_{min}) and as setpoint for the said output it uses the upper or lower voltage limit ($V_{lim,max}$ or $V_{lim,min}$), furthermore it acts relative to the desired test current I_{ref} and is naturally clamped to a value between 0 and 1 to assure that the system input is in the interval $[0,\ I_{ref}]$. In Figures 9 and 10 the layout and switching is illustrated.

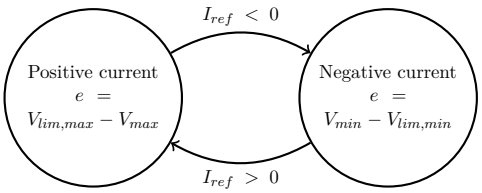

Figure 9. Illustration of the previously used regulators modes and switching.

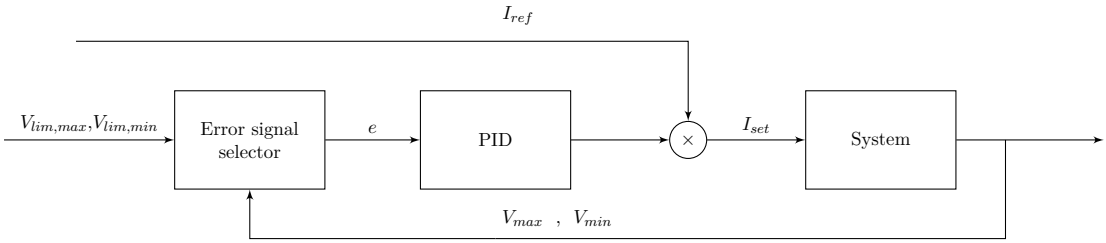

Figure 10. Layout of previous PID control. The analog parts of the system (battery and cycling equipment) is represented as one. Note that the desired current I_{set} may not be the actual system current I_{sys}.

Classic control theory approach As can be seen in Figure 5 the gain of the system does not drastically change within the operative area of the controller and the phase is not far from zero, thus a pure integrating controller will perform well. With classic control theory this could be extended to a first order control design, for example a PID with a lead/lag based method, and an improved compensation with regards to the cell dynamics could be achieved.

4.3 State space and transfer functions of cell model

Continuous time To analyse the system with more depth it is beneficial to formulate the system in form of a transfer function or a state space model, the cell model in Figure 4 can easily be written on state space form with Ohm's and Kirchhoff's laws together with the voltage-current relation for a capacitor. The capacitance is described by

$$I_{cap}(t) = c_{cap}\frac{dV_{cap}(t)}{dt} \tag{2}$$

where $I_{cap}(t)$ is the current through the capacitor and V_{cap} is the voltage across it, c_{cap} is the capacitance. Using V_{cap} as the state x, the cell current $I(t)$ as the input $u(t)$ and the cell voltage $V_{cell}(t)$ as the output $y(t)$ we have

$$x(t) = V_{cap}(t) \tag{3}$$
$$u(t) = I(t) \tag{4}$$
$$y(t) = V_{cell}(t). \tag{5}$$

With a state space model on the form

$$\dot{x}(t) = \mathbf{A}x(t) + \mathbf{B}u(t) \tag{6a}$$

$$y(t) = \mathbf{C}x(t) + \mathbf{D}u(t). \tag{6b}$$

we get

$$\mathbf{A} = -\frac{1}{R_2 c_{cap}} \quad , \quad \mathbf{B} = \frac{1}{c_{cap}} \quad , \quad \mathbf{C} = 1 \quad , \quad \mathbf{D} = R_1 \tag{7a}$$

The first order model works if the open circuit voltage $V_{OCV}(t)$ is constant and known. As the open circuit voltage changes considerably during the usage of the cell it needs to be considered for most control designs. If V_{OCV} is viewed as a linear function of the electrical charge, a model only valid for a small operational range, we can easily write a second order system. The charge is directly dependent on the current flow and thus V_{OCV} depends on the current through the cell

$$\dot{V}_{OCV}(t) = Ku(t). \tag{8}$$

with K as the voltage gain per time unit and current, one gets

$$x(t) = \begin{bmatrix} V_{cap}(t) & V_{OCV}(t) \end{bmatrix}^T \quad , \quad y = V_{cell}(t) \tag{9}$$

$$\mathbf{A} = \begin{bmatrix} -\frac{1}{c_{cap}R_2} & 0 \\ 0 & 0 \end{bmatrix} \quad , \quad \mathbf{B} = \begin{bmatrix} \frac{1}{c_{cap}} \\ K \end{bmatrix} \quad , \quad \mathbf{C} = \begin{bmatrix} 1 & 1 \end{bmatrix} \quad , \quad \mathbf{D} = R_1 \tag{10a}$$

The state space model can also be written as a transfer function in the Laplace domain, if transforming the model as in Equation (6) and rewrites it one gets

$$\mathbf{G}(s) = \mathbf{C}(s\mathbf{I} - \mathbf{A})^{-1}\mathbf{B} + \mathbf{D} \tag{11}$$

with $\mathbf{I}$ as the identity matrix. With the system as in Equation (10a) one gets the following transfer function

$$G_{cell}(s) = \frac{\frac{1}{c_{cap}}s + Ks + \frac{K}{R_2 c_{cap}}}{s^2 + \frac{1}{R_2 c_{cap}}s} + R_1 \tag{12}$$

which can also be written as

$$G_{cell}(s) = \frac{R_1 s^2 + (\frac{1}{c_{cap}} + K + \frac{R_1}{R_2 c_{cap}})s + \frac{K}{R_2 c_{cap}}}{s^2 + \frac{1}{R_2 c_{cap}}s}. \tag{13}$$

Discrete time approximations

By using a step length h and a forward difference approximation where

$$x(t+h) = x(t) + h\dot{x}(t) \tag{14}$$

one can produce a discrete time approximation of the state space model in both as in Equation (7a) and as in Equation (10a). Additionally, the transfer function can be approximated (using the same relation, Equation (14)) to the z-domain by the substitution

$$s \approx \tilde{s} = \frac{z-1}{h}. \tag{15}$$

The result (with $K = 0$) is

$$G_{cell}(z) = \frac{R_1 z^2 + (-2R_1 + h(\frac{1}{c_{cap}} + \frac{R_1}{R_2 c_{cap}}))z + R_1 - h(\frac{1}{c_{cap}} + \frac{R_1}{R_2 c_{cap}})}{z^2 + (-2 + \frac{h}{R_2 c_{cap}})z + (1 - \frac{h}{R_2 c_{cap}})} \tag{16}$$

The special case of including V_{OCV} as a state that does not change with input is selected as the open circuit voltage does change during usage, thus a preselected constant will have low accuracy. The included state for V_{OCV} actually represents all voltage contributions from reactions that are slower than what is modelled by the RC-circuit of the model.

Input-output model. The general basis for the discrete time parameter adaptation algorithms used in [10] is an input-output difference model on the form

$$y(t) = -\sum_{i=1}^{n_A} a_i y(t - ih) + \sum_{i=1}^{n_B} b_i u(t - dh - ih). \tag{17}$$

In our case the output at time t is directly affected by the input at t, which can be considered by allowing $d = -1$ or as in this case with a sum that starts at zero. After this change, a discrete time transfer function with the z-transform is written as

$$\frac{Y(z)}{U(z)} = G(z) = \frac{\sum_{i=0}^{n_B} b_i z^{-i}}{\sum_{i=0}^{n_A} a_i z^{-i}} \tag{18}$$

where $a_0 = 1$. With the second order model of a battery (Equation (16)) the corresponding input output model would be

$$y(t) = -a_1 y(t-h) - a_2 y(t-2h) + b_0 u(t) + b_2 u(t-h) + b_0 u(t-2h). \tag{19}$$

A relation between the direct parameters R_1, R_2, τ and indirect parameters a_i & b_i can easily be found. In the case with a second order system with a state representing

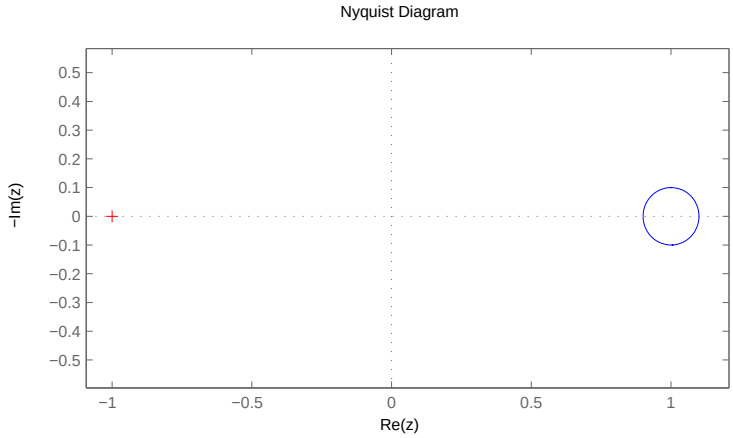

Figure 11. Example response of a cell model with the RC-part, in the form of a Nyquist plot.

the open circuit voltage (Equation (16)), i.e. $n_A = 2$, $n_B = 2$, we have

$$a_1 = -2 + h\frac{1}{R_2 c_{cap}} \tag{20a}$$

$$a_2 = 1 - h\frac{1}{R_2 c_{cap}} \tag{20b}$$

$$b_0 = R_1 \tag{20c}$$

$$b_1 = R_1[-2 + h(\frac{1}{R_1 c_{cap}} + \frac{1}{R_2 c_{cap}})] \tag{20d}$$

$$b_2 = R_1[1 - h(\frac{1}{R_1 c_{cap}} + \frac{1}{R_2 c_{cap}})]. \tag{20e}$$

4.4 Stability and robustness of the control

The cell, and the continuous time model of it, have states which are stable. From Equation (10a) it can easily be seen that the eigenvalues of the system matrix (the system poles) are located at $-\frac{1}{R_2 c_{cap}}$ and 0. The negative eigenvalue naturally corresponds to the state describing the capacitive part which is the fast behaviour within the model, this state is asymptotically stable and increasing the model order by adding additional capacitive parts will only add asymptotically stable states. If using the transfer function to the corresponding state:

$$G_{cell}(s) = \frac{R_2}{1 + sR_2 c_{cap}} + R_1 \tag{21}$$

and considering the Nyquist stability criterion [7, p. 76] one can see that value of $G_{sys}(i\omega)$ are located in the right half plane for all frequencies ω. In Figure 11 an example is shown with a high frequency gain of 0.9 and a low frequency gain of 1.1.

Thus the nyquist curve never encircles -1 and any control that does not bring the phase to -180 degrees will be stable with any positive gain. Thus, an integrating control would be stable for any gain in the ideal continous time system .

The sampling done by sensors transforms the closed loop into a discrete time system, this will have effects when applying the feedback. If any delay is introduced the phase of the system will be shifted as seen in Figure 5 and for any integrating control there will be an upper limit on the gain, if the system should be kept stable.

If considering the discrete time control the stability can be investigated by considering the Nyquist curve of $G_{\text{control}}(e^{i\omega})$ [8, p. 90-91]. A discrete time integrating control with gain K_I will have a transfer function of

$$G_{\text{control}}(z) = K_I \frac{h}{z-1} \tag{22}$$

we see that

$$G_{\text{control}}(e^{i\omega}) = K_I \frac{h}{e^{i\omega}-1} = K_I \frac{h}{\cos\omega + i\sin\omega - 1} = \frac{K_I h}{2}\left[-1 - i\frac{\sin\omega}{\cos\omega}\right]. \tag{23}$$

By considering the simple purely resistive model of a battery with resistance R a simple system can be analysed. The curve to consider is now

$$G_{\text{control}}(e^{i\omega})G_{cell}(i\omega) = \frac{K_I h}{2}\left[-1 - i\frac{\sin\omega}{\cos\omega}\right]\frac{1}{R} \tag{24}$$

and we clearly see that it only resides at the real value of $-\frac{1}{2}K_I h R$, thus we have a gain margin of $A_m = \frac{2}{K_I h R}$. The (in this case preferred) controller gain of $K_I = \frac{1}{Rh}$ will thus leave a gain margin of $A_m = 2$. When considering the model with time dependent parts, and also the response of the real cell, the changes from a pure resistance gain are not large and the simple gain margin as above still gives a good reference. A example of a nyquist plot of the system inluding an RC-part and a discrete time integrating control is shown in Figure 12. Similarly, it is a reference for controls methods that are close to the integrating controller. A conservative approach can also be taken with regards to stability of the real system, as an upper limit of the system gain can be considered.

4.5 Model based control

With a discrete model as in Equation (16) or in the form of Equation (17) a control that in theory brings the system to a desired output and holds it there is possible. The simplicity of the system makes methods such as model predictive control (MPC) trivial. If only considering the output at the next iteration a simple substitution of $y(t+1)$ for the desired output y_{ref} in Equation (28) and solving for $u(t+1)$ gives the sought input. For a system as in Equation (19) a control of

$$u(t+1) = \frac{1}{b_0}\left[y_{ref} - a_1 y(t) - a_2 y(t-1) + b_1 u(t) + b_2 u(t-1)\right] \tag{25}$$

brings the output to the desired level. As there is no desire to control the systems internal states and they are asymptotically stable there is no need consider them.

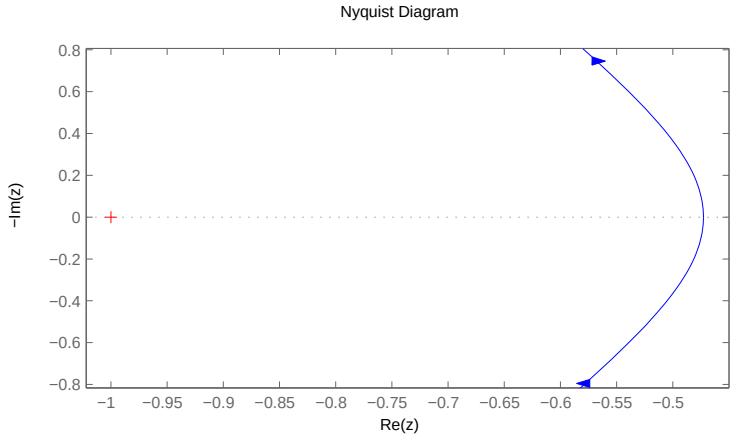

Figure 12. Example response of cell model with the RC-part and a discrete time integrating control with gain $K_I = 1/R_1$, in the form of a Nyquist plot.

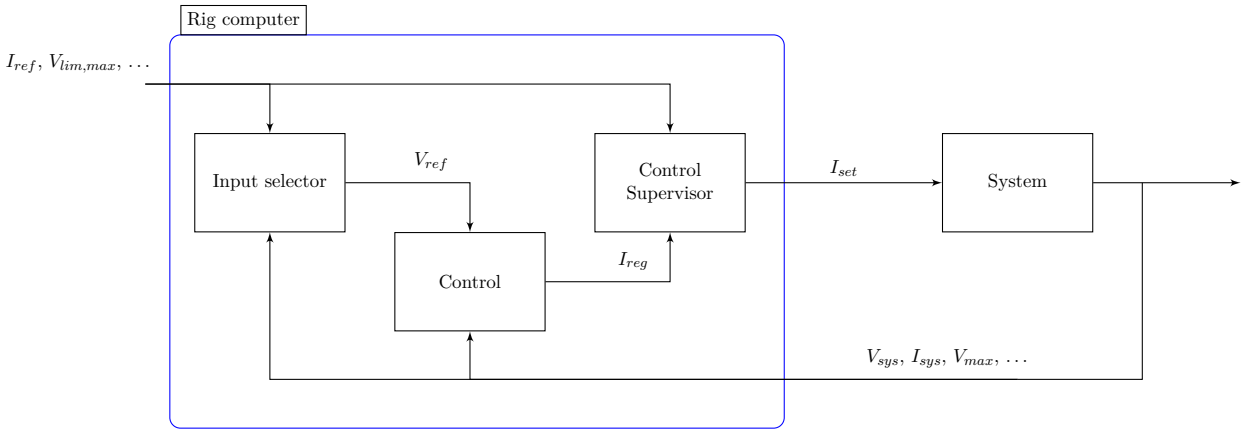

Figure 13. Block diagram of the general control layout.

4.6 Controller modes

As explained the input current is only to be controlled if any cell voltage limit is exceeded, and several possibilities for achieving this is possible. The goal is to keep the test and thus the current completely unaffected as long as no limit is exceeded. A solution to this is illustrated by Figures 13 to 15 and mainly consists of the control and a supervisor that is selecting what input to use. Some of the logic is the same as used before, in Figure 14 an corresponding selection of upper or lower limit is illustrated. A logic to select when the controller should be active is also implemented. Basically, the control is always active and a supervisor decides if the control setpoint for the current is to be used or if the reference current should be used. The conditions for this switching is illustrated in Figure 15.

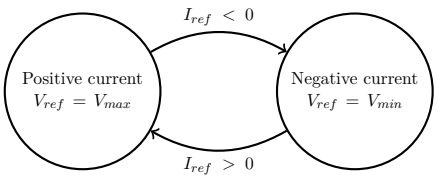

Figure 14. Illustration of the input selectors and switching.

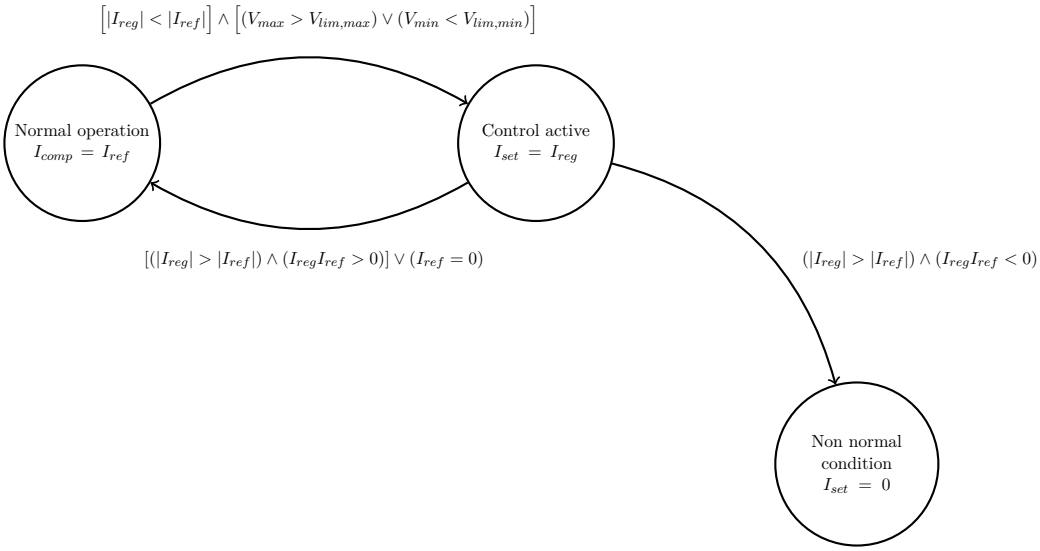

Figure 15. Illustration of the modes of the supervisor and its switching.

5 Adaptive control

As explained in Section 1 the problem is to control the system during dynamic changes that occur. As seen in Section 3.3 the changes in the system during the different conditions are major, but from classic stability theory we see that it is possible to design a simple controller such as an integrating feedback that is stable for all external conditions by leaving a large enough gain margin. This will however affect the performance of the controller, which in step responses are seen mainly as a large rise time. To achieve good and consistent performance along the full operational window without detailed knowledge of the cells (or retuning during usage) an adaptive control is designed, in other words a self tuning controller.

Adaptive or self tuning controllers have been used for a long time, an early coverage of this topic is given in [9], and today common methods are described in [10] and other books. More specific methods of different kinds have certainly been investigated before.

In our application the adaptation is a means of handling the changes in impedance during, for example, different temperatures. Partly because the exact dynamics of

the battery system are not known, one of the purposes of the test rig (in which the control is to be implemented) is to determine these kinds of parameters exactly. But another important objective is to design a control that is not in need of major retuning if changing battery systems. An original requirement was to have at most one single parameter that needs to change during change of battery systems, with an adaptive method there is a possibility for a completely autonomous control.

In Section 4.5 we see that an optimal control can be designed for the model with certain assumptions and a set of known parameters for the model (as in Section 3). By using previous measurements these parameters can be determined and with a recursive algorithm it can be implemented and used within the control computer.

5.1 Adaptation algorithms and recursive least squares

The recursive parameter adaptation algorithm used is based on [10, p. 61-] and is on the form

$$\theta(t+1) = \theta(t) + f(\theta(t), \phi(t), \epsilon(t)) \tag{26}$$

where $\theta(t)$ is the current set of parameters at time t, $\phi(t)$ is our measurements and $\epsilon(t)$ is the prediction error. By rewriting Equation (17) on vector form, with

$$\theta(t) = \begin{bmatrix} -a_1 \\ -a_2 \\ \vdots \\ -a_{n_A} \\ b_0 \\ b_1 \\ \vdots \\ b_{n_B} \end{bmatrix}, \quad \phi(t) = \begin{bmatrix} y(t) \\ y(t-1) \\ \vdots \\ y(t-n_A) \\ u(t+1) \\ u(t) \\ \vdots \\ u(t-n_B) \end{bmatrix}, \tag{27}$$

one can separate a parameter vector $\theta(t)$ and a measurement vector $\phi(t)$ and get the relation

$$y(t+1) = \theta(t)^T \phi(t). \tag{28}$$

and also define the *prediction error* at each time step t

$$\epsilon(t) = y_{measured}(t) - \theta(t)^T \phi(t-1). \tag{29}$$

Note that this definition considers the prediction of the output at time t, with the parameters at time t. Called the posteriori prediction error, not to be confused with the priori prediction error.

The correction of the parameters, $f(\theta(t), \phi(t), \epsilon(t))$, that determines the new parameter set $\theta(t+1)$ at each discrete step determines the properties of the algorithm. If one wants to minimize the size of the prediction error one can make a distinction between what is denoted prior and posterior prediction error and then specify a

quadratic function

$$J(t) = \sum_{i=1}^{t}(y(t) - \hat{\theta}(t)^T\phi(t-1))^2 = \sum_{i=1}^{t}(\epsilon(t))^2. \tag{30}$$

where $\hat{\theta}(t)$ is a new set of parameters to be used. This is minimized with regards to $\hat{\theta}(t)$ by considering the value where

$$\frac{\delta J(t)}{\delta\theta(t)} = \sum_{i=1}^{t}(y(t) - \hat{\theta}(t)^T\phi(t-1))\phi(t-1) = 0 \tag{31}$$

and together with knowing that

$$(\hat{\theta}(t)^T\phi(t-1))\phi(t-1) = \phi(t-1)(\hat{\theta}(t)^T\phi(t-1))^T = \phi(t-1)\phi(t-1)^T\hat{\theta}(t) \tag{32}$$

one gets

$$\sum_{i=1}^{t}\phi(t-1)\phi(t-1)^T\hat{\theta}(t) = \sum_{i=1}^{t}y(t)\phi(t-1) \tag{33}$$

To get a recursive algorithm one defines

$$F(t)^{-1} = \left[\sum_{i=1}^{t}\phi(t-1)\phi(t-1)^T\right] \tag{34}$$

and thus gets

$$F(t)^{-1}\hat{\theta}(t) = \sum_{i=1}^{t}y(t)\phi(t-1) \tag{35}$$

or

$$\hat{\theta}(t) = F(t)\sum_{i=1}^{t}y(t)\phi(t-1). \tag{36}$$

By considering

$$\hat{\theta}(t+1) = F(t+1)\sum_{i=1}^{t+1}y(t)\phi(t-1). \tag{37}$$

$$\hat{\theta}(t+1) = F(t+1)\left[y(t+1)\phi(t) + \sum_{i=1}^{t}y(t)\phi(t-1)\right] \tag{38}$$

and inserting Equation (35)

$$\hat{\theta}(t+1) = F(t+1)\left[y(t+1)\phi(t) + F(t)^{-1}\hat{\theta}(t)\right] \tag{39}$$

and correspondingly considering

$$F(t+1)^{-1} = \sum_{i=1}^{t+1}\phi(t-1)\phi(t-1)^T \tag{40}$$

$$F(t+1)^{-1} = \phi(t)\phi(t)^T + \sum_{i=1}^{t} \phi(t-1)\phi(t-1)^T \tag{41}$$

$$F(t+1)^{-1} = \phi(t)\phi(t)^T + F(t)^{-1} \tag{42}$$

$$F(t)^{-1} = F(t+1)^{-1} - \phi(t)\phi(t)^T \tag{43}$$

and inserting this into Equation (39)

$$\hat{\theta}(t+1) = F(t+1)\left[y(t+1)\phi(t) + F(t+1)^{-1}\hat{\theta}(t) - \phi(t)\phi(t)^T\hat{\theta}(t)\right] \tag{44}$$

$$\hat{\theta}(t+1) = \hat{\theta}(t) + F(t+1)\phi(t)\left[y(t+1) - \hat{\theta}(t)^T\phi(t)\right] \tag{45}$$

and we arrive at our parameter update function by using $\hat{\theta}(t+1)$ as our new parameters. Thus we use (with Equation (29))

$$\theta(t+1) = \theta(t) + F(t+1)\phi(t)\epsilon(t) \tag{46}$$

where $F(t+1)$ is called adaptation gain, in general a square matrix ($[n_A+n_B+1]\times[n_A+n_B+1]$) or a scalar, in this case a matrix that is updated with the algorithm

$$F(t+1)^{-1} = F(t)^{-1} + \phi(t)\phi(t)^T \tag{47}$$

which with the matrix inversion lemma can be show to be equivalent to

$$F(t+1) = F(t) - \frac{F(t)\phi(t)^T\phi(t)F(t)}{1+\phi(t)^TF(t)\phi(t)}. \tag{48}$$

This is shown in detail within [10, p. 64] together with several update algorithms. The basic selection of gain may be modified depending on the desired behaviour, common is to include two weights $\lambda_1(t)$ and $\lambda_2(t)$:

$$F(t+1)^{-1} = \lambda_1(t)F(t)^{-1} + \lambda_2(t)\phi(t)^T\phi(t) \tag{49}$$

which implies

$$F(t+1) = \frac{1}{\lambda_1(t)}\left[F(t) - \frac{F(t)\phi(t)^T\phi(t)F(t)}{\frac{\lambda_1(t)}{\lambda_2(t)} + \phi(t)^TF(t)\phi(t)}\right]. \tag{50}$$

With a simple selection of weights where $\lambda_1 < 1$ and $\lambda_2 = 1$ have the result of minimizing

$$J(t) = \sum_{i=1}^{t} \lambda_1^{t-i}\epsilon(t)^2 \tag{51}$$

and a similar recursion as from Equation (30) can be done. This is often called using a *forgetting factor* as one puts less value on old values than new and is shown in detail within [10, p. 68].

This can be extended by considering the model parameters as a dynamic system and introducing certain assumptions, particularly adding disturbances in form of Gaussian white noise, and subsequently one can formulate an update algorithm using the optimal Kalman gain. In [10, p. 72-75] this is done with an algorithm as above, with similar results and a slightly different update of the parameters. This method can in special cases be interpreted as factors λ_1 and λ_2 that are based on the covariance of the noise. In practice the selection of λ_1 is based on how the system is excited, in our case we have short periods of input in form of current and longer periods of input consisting of noise in the input that excites the system but at a amplitude that largely differs from usage. This small amplitude input does help the convergence to a certain degree but the parts of the system that is significantly exited differs from the model that is valid for larger input currents as a result of unmodelled dynamics and non-linear behaviour. Thus we select a λ_1 that is small enough to have quick convergence in case of changes in the system during periods with no input that excites the system, but not so small that the gain increases during normal testing with pulses.

5.2 Parameter adaptation convergence

The algorithm described by Equations (29), (46) and (47) with the system as in Equation (28) is in [10] shown to be asymptotically stable for any initial value of the gain $F(t_0) > 0$, by using the principle of system passivity. In addition to stability it is shown in [10, p. 116] that under the following conditions:

1. The parameter adaptation algorithm is stable
2. The orders n_A and n_B of the system to be identified are known exactly
3. The system to be identified is characterized by an irreducible transfer function in z
4. The input u(t) is a *persistently exciting signal* of order $n = n_A + n_B$.

A signal $u(t)$, is said to be *persistently exciting* of order n if

$$\lim_{t_1 \to \infty} \frac{1}{t} \sum_{t=1}^{t_1} \phi(t)\phi(t)^T > 0 \tag{52}$$

with $\phi = \begin{bmatrix} u(t) & u(t-1) & \cdots & u(t-n+1) \end{bmatrix}$. It also shown that $u(t)$ is a persistently exiting signal for all non-zero polynomials $L(z)$ of order $n-1$ if

$$\lim_{t_1 \to \infty} \frac{1}{t} \left[\sum_{t=1}^{t_1} L(z)u(t) \right] > 0. \tag{53}$$

For practical usage this implies that the input signal needs to be composed of at least n distinct frequencies.

In the practical application on HPPC testing the convergence conditions above are not fulfilled. Mainly the system is of a high unknown order, and additionally the input signal is not necessarily persistently exciting of a high enough order if considering a limited time horizon. This does however not mean that results are not satisfactory. The battery system to be identified does have distinct behaviours that can be modelled with a known order under a limited operational window. In practice the modelled order reflects the number of measurement points that are considered, and together with the sampling time the adapted model will mainly reflect behaviours that have significant importance within this time region. The unmodelled dynamics do introduce some difficulties, and there are some undesired results. One way to handle this is covered in [11] by introducing a value on the information content in the current signal which depends on the system excitation. Another modification is to project the parameters a_i and b_i onto a smaller set of plausible parameters. In this case we have a bounded three dimensional room defined by Equation (20) and reasonable values of R_1, R_2 and τ. In simulations this projection did not help convergence to a significant extent and in some cases the performance was decreased.

Modifications and usage

To ensure the robustness of the control and the adaptation a number of additions can be added in practical use, most importantly during the convergence of the parameters. To ensure that the controlled system will never be unstable during this early period one can use a pure integrating control with a sufficiently low gain to ensure stability, or introduce an additional safety factor that increases the gain margin. Switching to the higher performing control can be done based on either the model prediction error, the value of the gain F, or based on a comparison between two or more models with different configurations. The last alternative was selected for testing, as different initial values could be selected, corresponding to a high and a low system gain. During normal convergence this results in only using a low gain margin while the adapted parameters represent an accurate system.

6 Implementation and evaluation

6.1 Adaptation convergance

The adaptation algorithms and the control were initially evaluated by simulations in MATLAB using Simulink. The recursive least squares method with the additional forgetting factor were implemented in both simulations and the test rig. In the simulations models of different order were evaluated, of reasonably low order. Experiments with up to a fifth order system were done, but as the basic cell model is only linked to a second order input output function ($n_A = 2$, $n_B = 2$) this was used

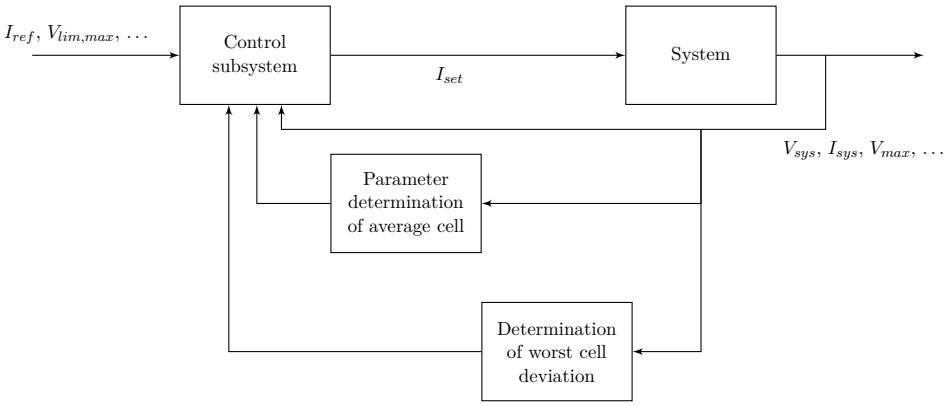

Figure 16. General layout of the adaptive parts of the control.

in the experiments, together with the purely resistive model. The simulations were run against static data from previous testing of different forms, and one can expect results close to would be achieved in real system testing. One limitation was that earlier test data were recorded with 10Hz sample rate, hence the algorithm used in simulation was tested with the same rate, while the intended time step is based on the measurement rates, i.e. up to 50Hz.

Simulations

Initially, an adaptation to a single parameter model (based on a cell with only a resistive part) is performed. In Figure 17 this is shown and the convergence is fast, as it is not easy to determine the true value it is not trivial to measure the exact performance. The initial values for the parameter used in Figure 17 are about ten times above the expected value, and at the first system input the adapted resistance quickly reaches a reasonable value around 3.7 and then decreases slightly with each change in current, i.e. each input that excites the system. The temperature increases during the test and we can assume that the decrease in the resistive parameter is a result of this. Similar outcomes are seen in simulations based on other data and generally the result of the adaptation to a purely resistive model of the battery is good for all usage cases.

In Figure 18 a simulation of a five parameter adaptation is shown from a typical set of current pulses, thus the input to the system is a current I_{sys} with a set of discrete changes in addition to noise. The changes in current can clearly be seen in the convergence of the parameters as rapid changes. If considering the parameter $b_0 = R_1$ we can see that it quickly reaches a value close to what can be assumed correct (in this case just above 3.5 at the start of testing). During the test this parameter decreases, which (as previously) is probably linked to the increase in temperature during usage of the battery system.

In Figure 19 the interpretation of the parameters a_i and b_i in form of resistances

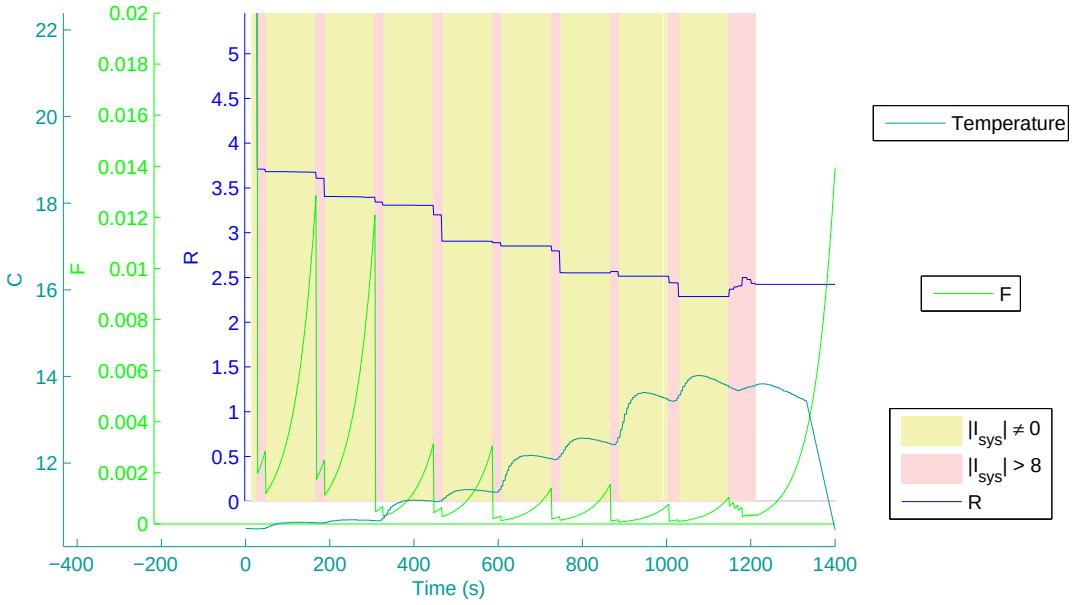

Figure 17. The single parameter R and the corresponding gain F. During adaptation of internal resistance in a simulation with data based on a pulse test, the resistance is normalized as in Figure 6. Asa a reference the temperature is shown as well as the periods with small or large system input.

R_1, R_2 and the time constant τ is shown, calculated with the equation system formed by Equation (20). The system is overdetermined but we see that $a_1 + a_2 \approx -1$ and $b_0 + b_1 + b_2 \approx 0$ as expected, and the adaptation follows the physical model.

If considering a_1,a_1,b_1 and b_2 or the corresponding τ and R_2 we notice two behaviours. One is the large discrete changes of a parameter, only to quickly return. This is most likely a result of a large delay in some measurement or a dropped package. The other is the cyclic behaviour of the parameters, during a large change in the current input the parameters τ and R_2 rises, but during constant current they slowly decay. This result is an indication of different parts of the system being significantly excited at different inputs. The different inputs beeing either a significant (desired) variation in current, or a small (undesired) variation that is regarded as noise. This is undesired and the magnitude of this effect may be changed by selecting an appropriate gain, in this case the changes in current is approximately twice every 100 seconds, a forgetting factor $\lambda_1 = 0.998$ is selected, resulting in a weight of around 0.135 on values from 100 seconds ago. Selecting a smaller λ_1 results in more noise propagating through to the parameters. By increasing λ_1 one can stabilize the parameter adaptation, as shown in Figure 20, but if considering the prediction error ϵ we see a negative effect.

The mean value and standard deviation of the prediction error ϵ for different values of λ_1 is shown in Table 1. The mean value is expected to be close to zero while

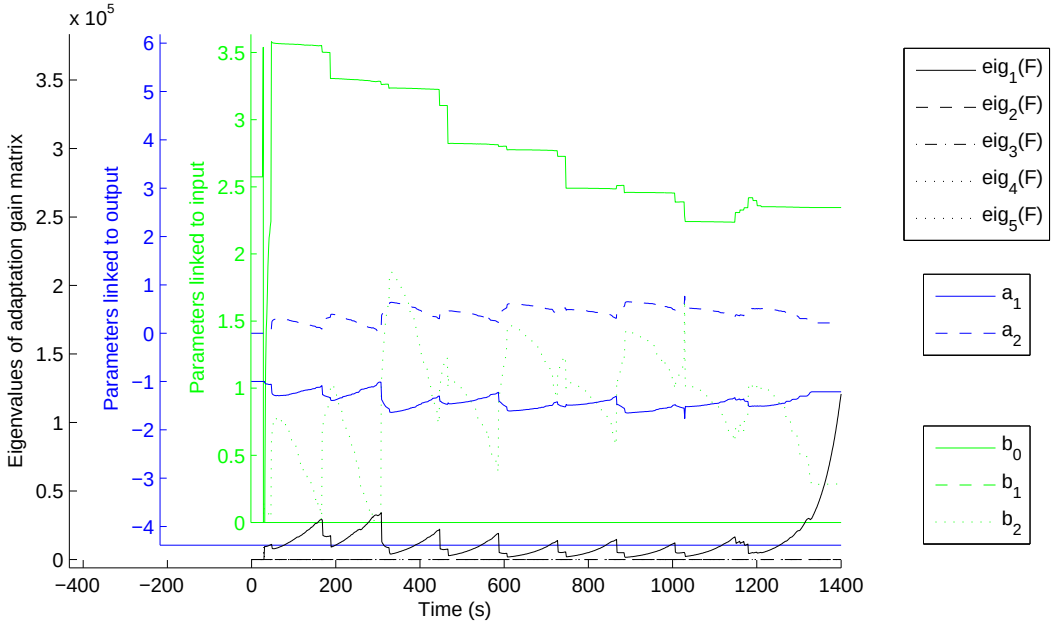

Figure 18. The five parameters in the adaptation as functions of time during a simulation based on a pulse test, the parameters b_i are normalized with the same resistive value as previously. $\lambda_1 = 0.998$.

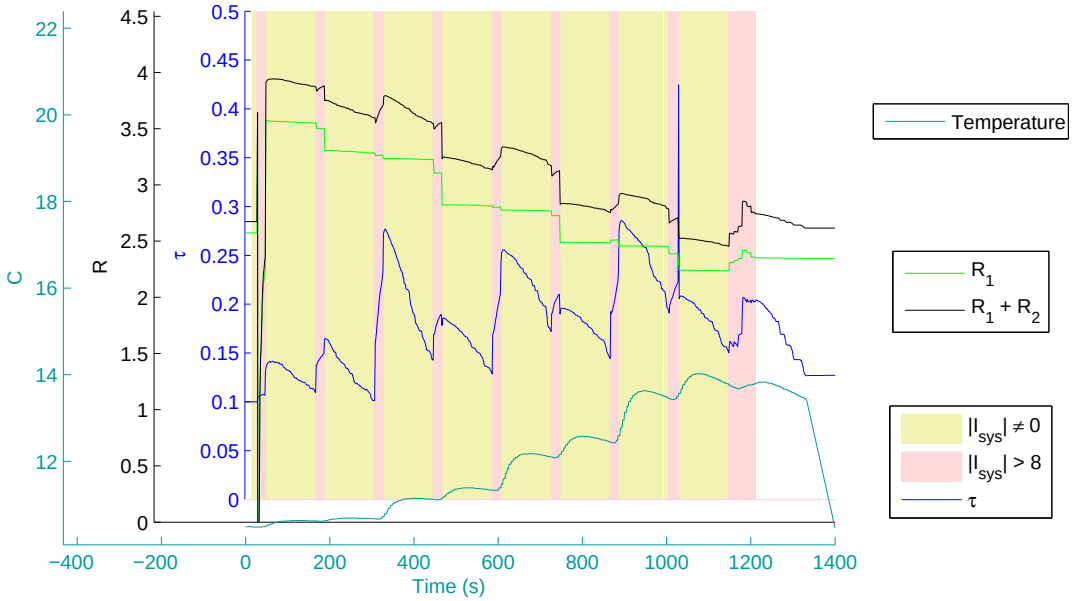

Figure 19. The interpretation of the parameters a_1,a_2,b_0,a_1 and b_2 from Figure 18 in form of resistance values R_1,R_2 and a time constant τ.

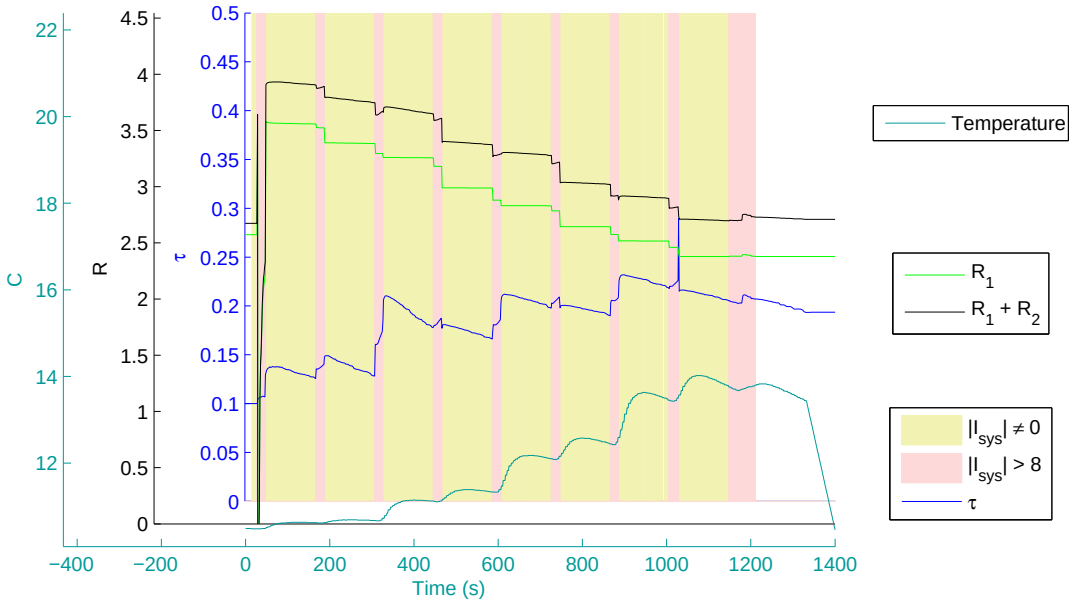

Figure 20. Values of R_1,R_2 and a time constant τ from a simulation with $\lambda_1 = 0.9995$.

	$\lambda_1 = 0.98$	$\lambda_1 = 0.998$	$\lambda_1 = 0.9995$
mean value $[10^{-6}]$	-0.000042	-8.0	-10.0
standard deviation (10^{-6})	626.4	579.9	620.6
mean value (close to voltage limit) $[10^{-6}]$	-89.4	-110.9	-126.8
standard (close to voltage limit) $[10^{-6}]$	628.0	589.0	719.4

Table 1. Performance of prediction during adaptation in form of standard deviation of the one step prediction error ϵ, in values in cells are to be interpreted as microvolts (10^{-6} V) although the original values used are normalized with a factor that is only close to one.

the standard deviation gives a size on the usual error, additionally the said values are calculated for a subset of sample points when the cell voltage is close to the limits $V_{lim,max}$ or $V_{lim,min}$. This gives an idea of the performance of the parameters when regulation would be active. The negative mean value of the prediction error is likely a result of a smaller distance to the upper cell voltage limit than to the lower, i.e. $|V_{lim,max} - V_{OCV}| < |V_{lim,min} - V_{OCV}|$. With the result that the error is more often considered during positive currents.

In Figure 21 the result of a simulation with input that is selected from a test based on actual drive cycles, the system input and output is shown in Figure 22. In this case the input is not as periodic, and we see a more continuous behaviour of the parameters. We also note that, in periods, the second resistance R_2 takes values around zero and the improvement of the added RC-circuit part of the model

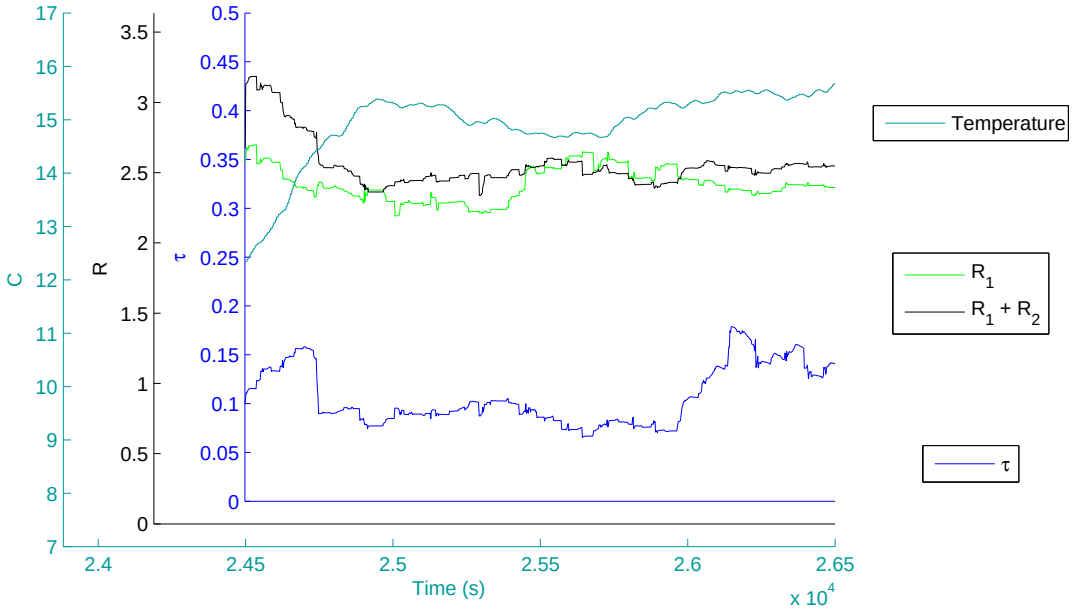

Figure 21. Convergence of parameters in simulation with input based on drive cycle testing.

is questionable. The cause of this might for example be dynamics in the system originating in other parts than the cells, possibly filtering of raw measurement data.

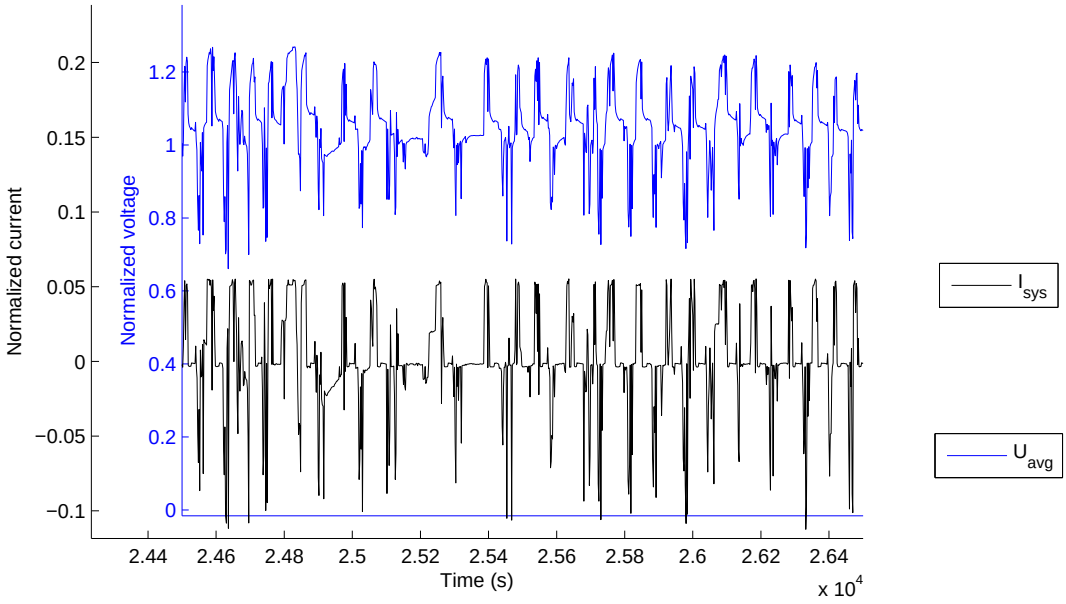

Figure 22. Input used during a test based on drive cycle usage.

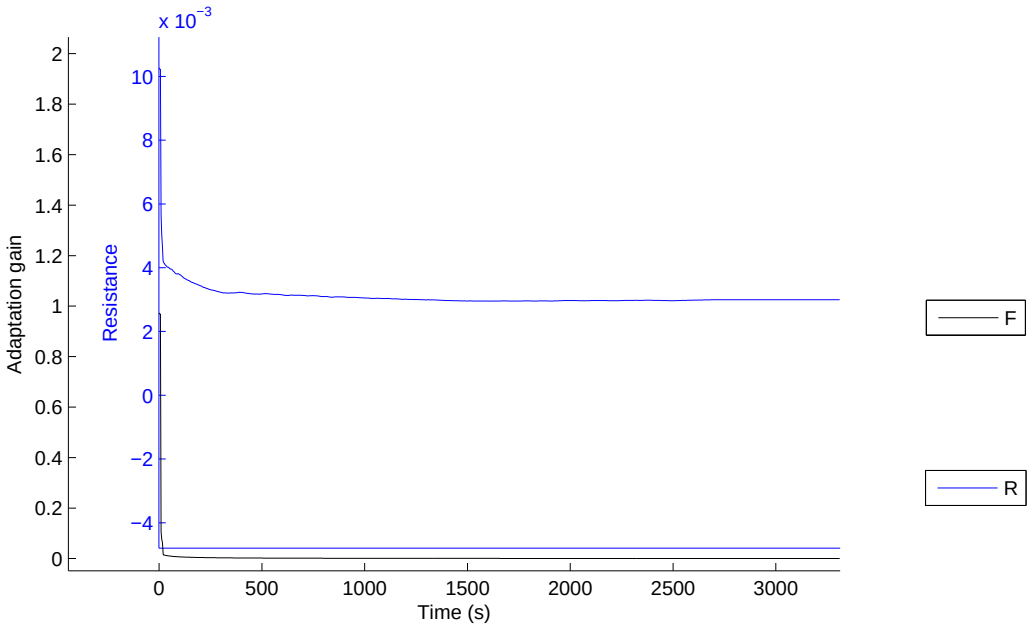

Figure 23. Typical convergence of a single parameter model from starting values during usage in testing. The system excitation mainly consist of a discrete disturbance at the beginning as a result of system activation and a current step as a start of setting the system in the desired state. Additionally there are continuous disturbances from the actuator on the system input I_{sys} that excites the system, the input and output is shown in Figure 25.

Testing

In Figures 23 and 24 some results of convergence during usage is shown, using 50Hz as the sampling frequency. Most testing start with limited excitation of the system, but disturbances and just a single step excites the system enough for the algorithm to gain information about the absolute value of the impedance around the sampling frequency. The input for the said results is shown in Figure 25. In these results we can see that the parameters in form of resistances and a time constant quickly reaches a stable value. If considering the capacitive part of the model we see that the higher sampling frequency makes the modelled second resistance take even smaller values, and the system as viewed from the adaptation algorithm drifts further from a typical battery.

If considering the parameters in a pulse test with relatively high excitation of the system, as a result of small delays between changes in current amplitude we see similar results as earlier for the 50Hz adaptation. However, if the sampling frequency is lowered to 10Hz as in Figure 27 there is a clear positive value on R_2. A comparision between different sampling frequencies is shown in Figures 26 and 27. The shorter time span considered by the adaptation algorithm at a higher sampling frequency generally makes the time dependant behaviours of the cell invisible, this

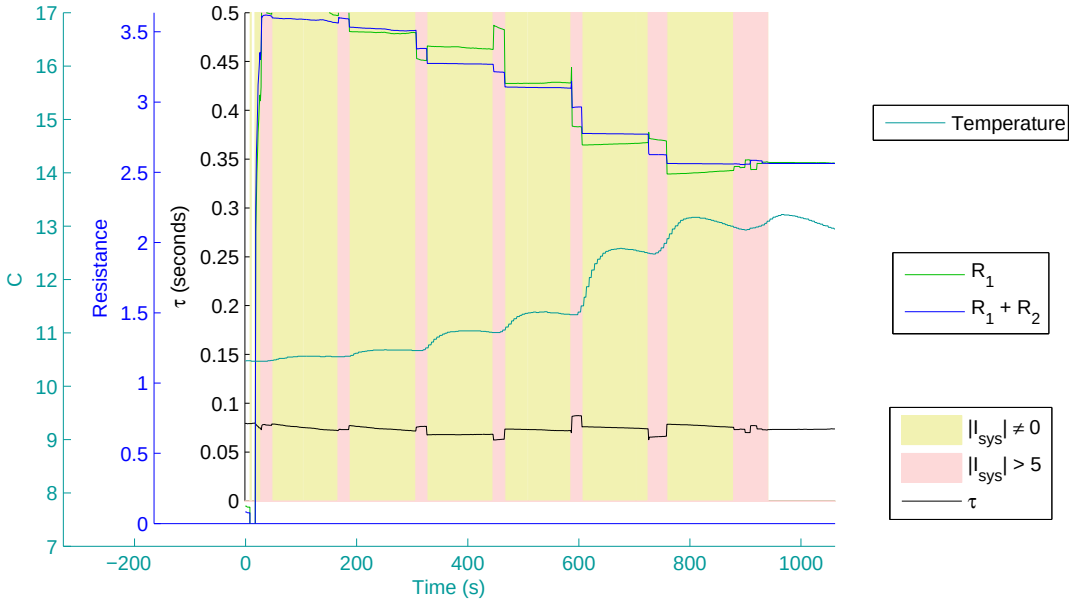

Figure 24. Typical convergence of a second order model from starting values during usage in testing. Input as in Figure 25.

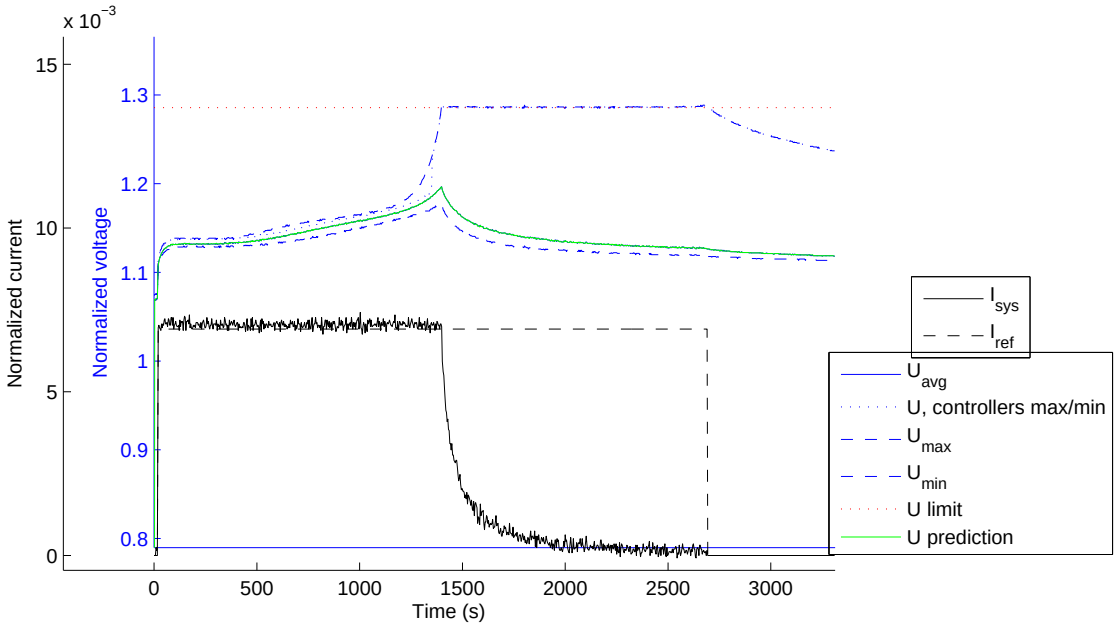

Figure 25. Typical input to the system during a test start.

may partly be a result of the dynamics in the actuator that limits the excitation of the higher frequency dynamics of the cell.

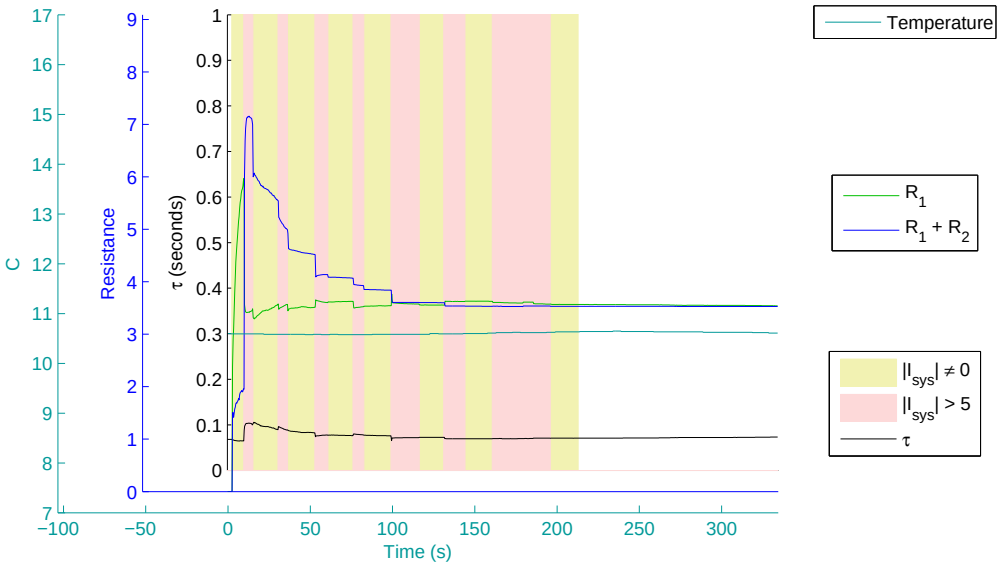

Figure 26.

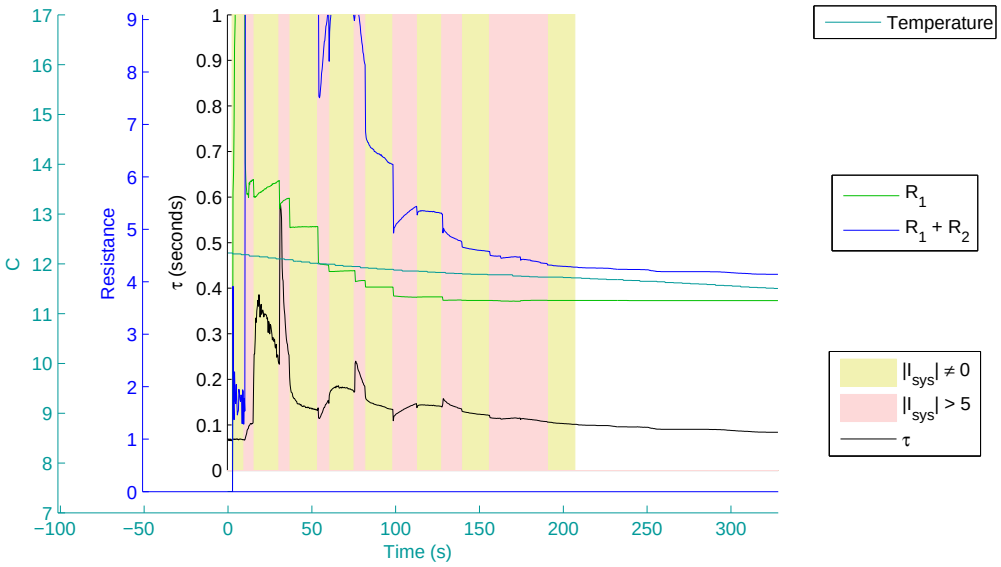

Figure 27.

6.2 Control performance

The control were simulated against a model based on the same theoretical knowledge used for the regulator design. In the ideal case the control can perfectly select a value on the current that puts the voltage on the limit, and thus the result follows the assumptions on parameter precision, delay and noise. As the ideal control has a gain margin of $A_m = 2$, and it is based upon previous values of the system input rather than internal states, the closed loop is stable even under large delays and considerable uncertainties.

The simulations were followed by implementation of the algorithms in the LabView environment used within the test rigs. In addition a simple model for simulation within LabView were programmed for reasonable testing of the LabView code before live usage.

Initially the response of the previously used control were tested to get a reference for the type of improvement achieved. In Figures 28 and 31 the result of reaching a voltage limit with the previous control is shown, together with the values in form of settling time and overshoot in Table 2. The definition of rise time and settling time is based on 10% and 2% of a typical voltage step, since the step in the reference current is not directly related. As some current steps does not result in a voltage step that exceeds the limit some values are set to zero. More specifically, if the voltage never exceeds the limit by more than 10% or 2% the rise time or settling time are defined to be zero.

In Figures 29 and 30 a step in current and the resulting control is shown (with the newly implemented controller). By design the current rises until the voltage limit is exceeded. The step response is shown in the same time-scale as the previous figures (for performance comparison with the previous control) together with a zoomed one. The effect of delays are clearly seen, and as a result there is an uncompensated rise in voltage of the cell. This rising voltage is linked to a time dependant effect that is not seen by the adaptation algorithm as it only considers a limited time horizon. If considering control during voltage saturation (Figures 32 and 33) the control is close to ideal, as the overshoot is in the same size as the precision of the voltage measurement. Some examples of the performance in form of common step response values are seen in Table 2 compared to the equivalent values of the previous controller.

Generally the response of the control is good with regards to the purely resistive value of an average cell, but with data from a limited time interval and delays in the system there are noticeable time dependant effects that is not compensated for. Additionally there is a large performance loss due to the delay in the individual cell voltage measurements, this is however of smaller amplitude as the cells are generally similar and previous deviation values are used with some precision before feedback is received.

When considering the response during a test with input based on drive cycles, using limits that are often exceeded (Figure 34), the performance is better than in the case with pulse tests. This is a result of an adaptation algorithm having more

	Old control				
	Charge saturation	Saturation 1 (Figure 31)	Step 1 (Figure 28)	Saturation 2	Step 2
overshoot	0.0093	0.0057	0.0357	0.0057	0.035
rise-time	0	0	5.8000	0	6.1000
settling time	35.1800	9.4800	12.3800	7.1800	11.9800

	Improved control				
	Charge saturation	Saturation 1 (Figure 32)	Step 1 (Figure 29)	Saturation 2	Step 2
overshoot	0.0036	0.0014	0.0136	0.0014	0.0329
rise-time	0	0	0	0	0.2000
settling time	0	0	1.7800	0	1.4800

Table 2. Examples of control performance, old and improved control respecively.

information for the cell parameters and the deviation between the average and worst cell. There is a clear delay between the regulators action and the system input that is also an important limiting factor. In Figure 35 an example of this delay is shown, the controllers output I_{set} is shown along with the system current I_{sys}.

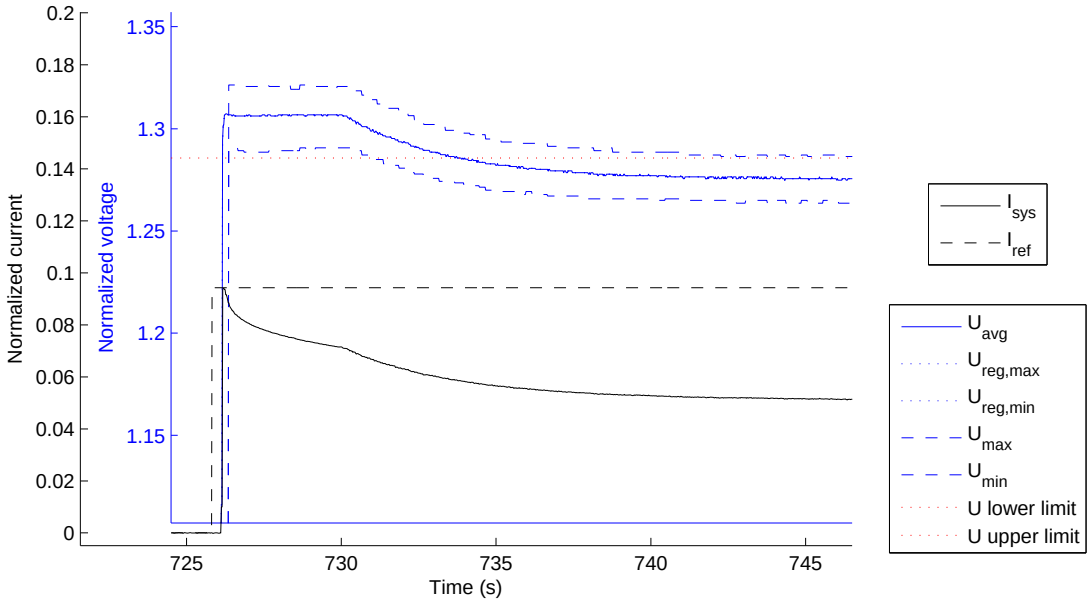

Figure 28. Response of previously used control, during a step in current. Comparison with Figure 29.

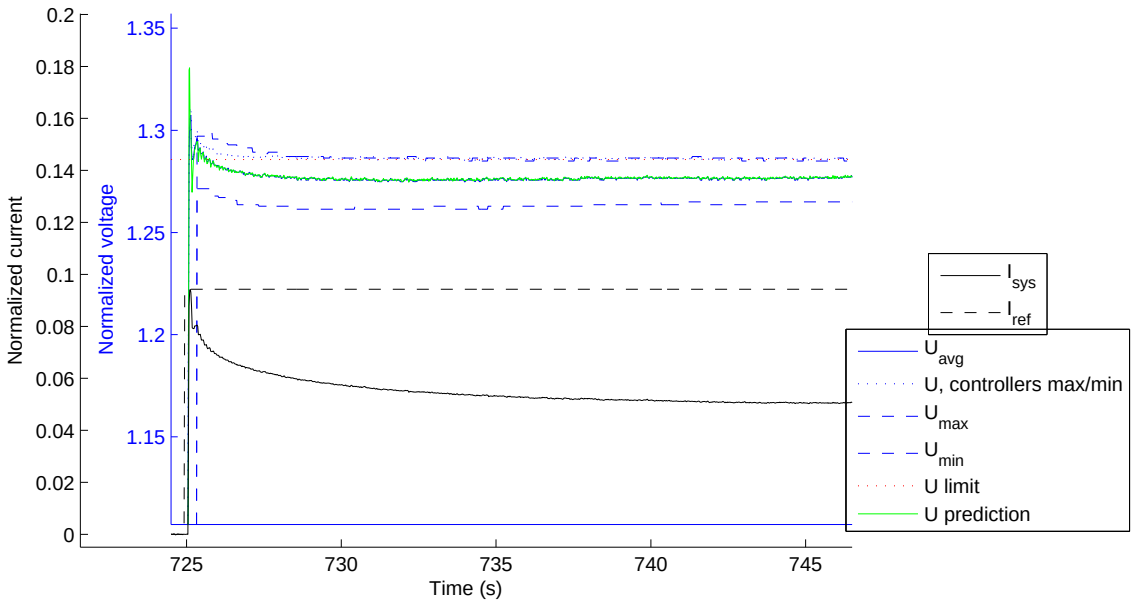

Figure 29. A step in I_{ref} with active control occurring during a pulse test. The average cell with the active offset is also shown with dots, this is to be interpreted as the controllers estimated extreme voltage. The controllers prediction of the average voltage is also shown, as a reference for the accuracy of the parameters. Comparison with Figure 28.

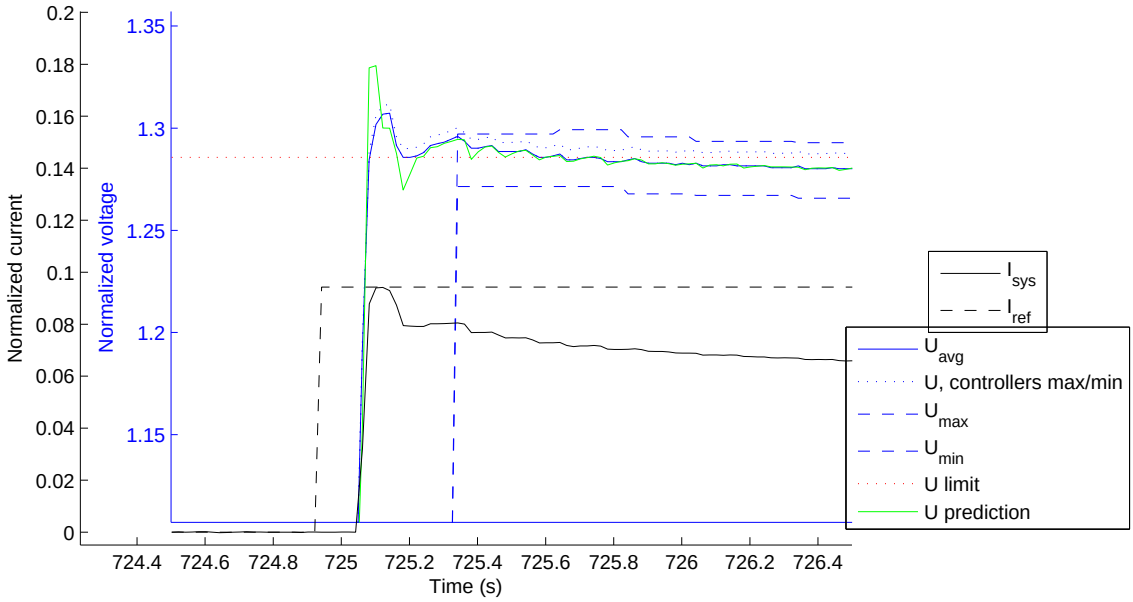

Figure 30. Same data as in Figure 29 but with different timescale, to view the details.

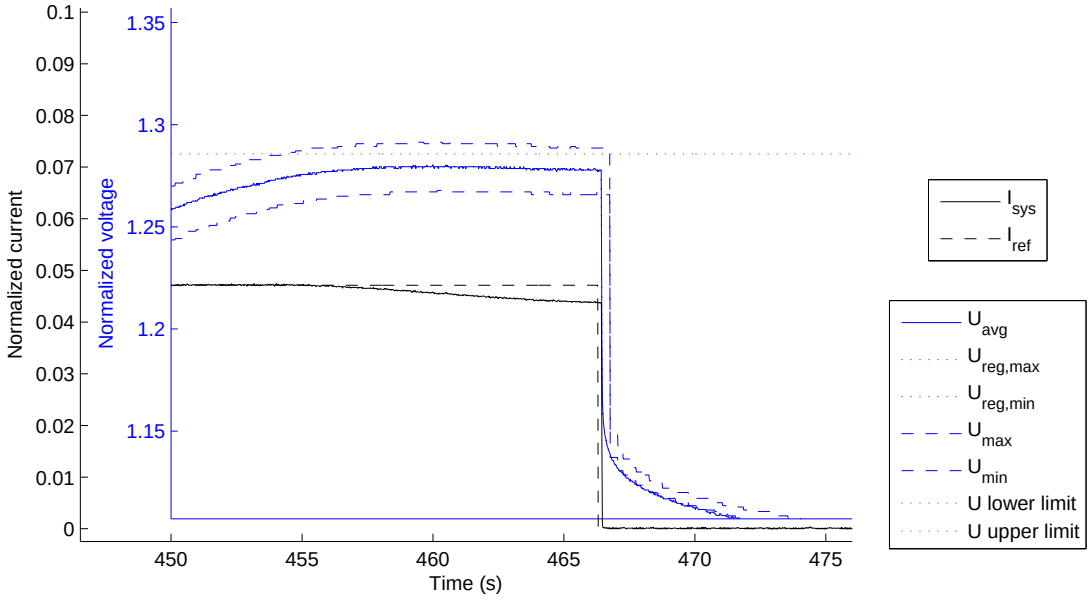

Figure 31. Response of previously used control, during voltage saturation, comparison with Figure 32.

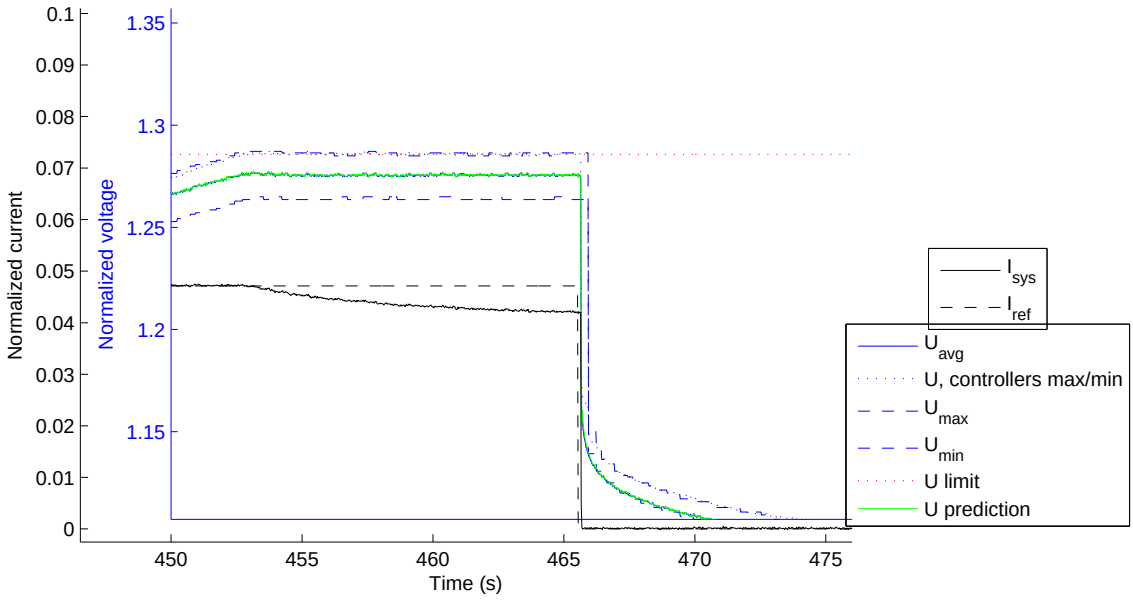

Figure 32. Increasing potential resulting in active control during a pulse test, comparison with Figure 31

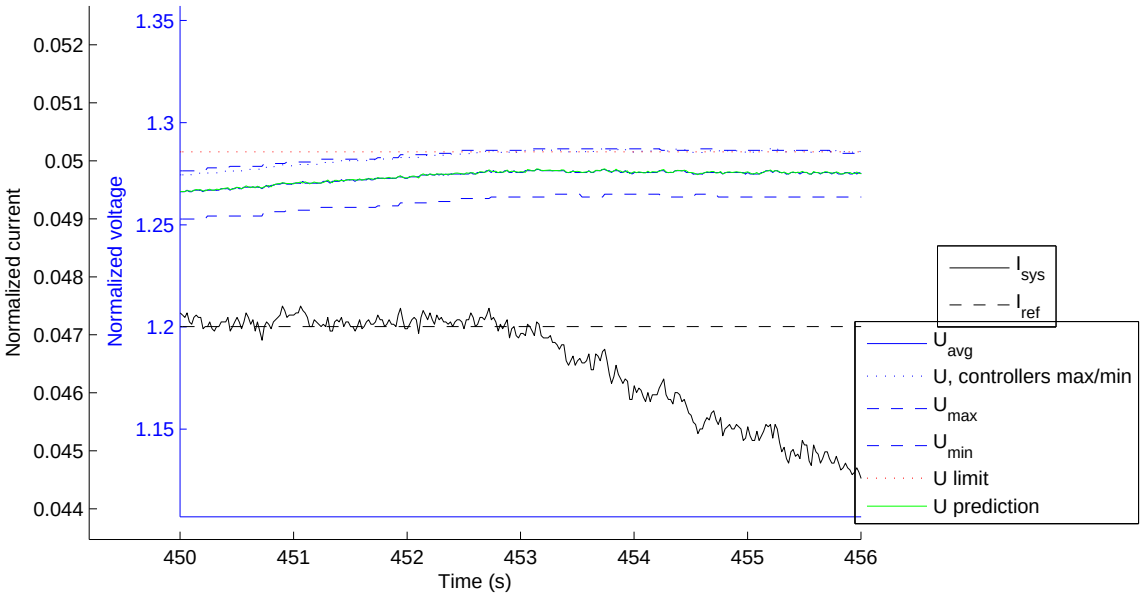

Figure 33. Increasing potential resulting in active control during a pulse test. Same data as in Figure 32 but with different timescale.

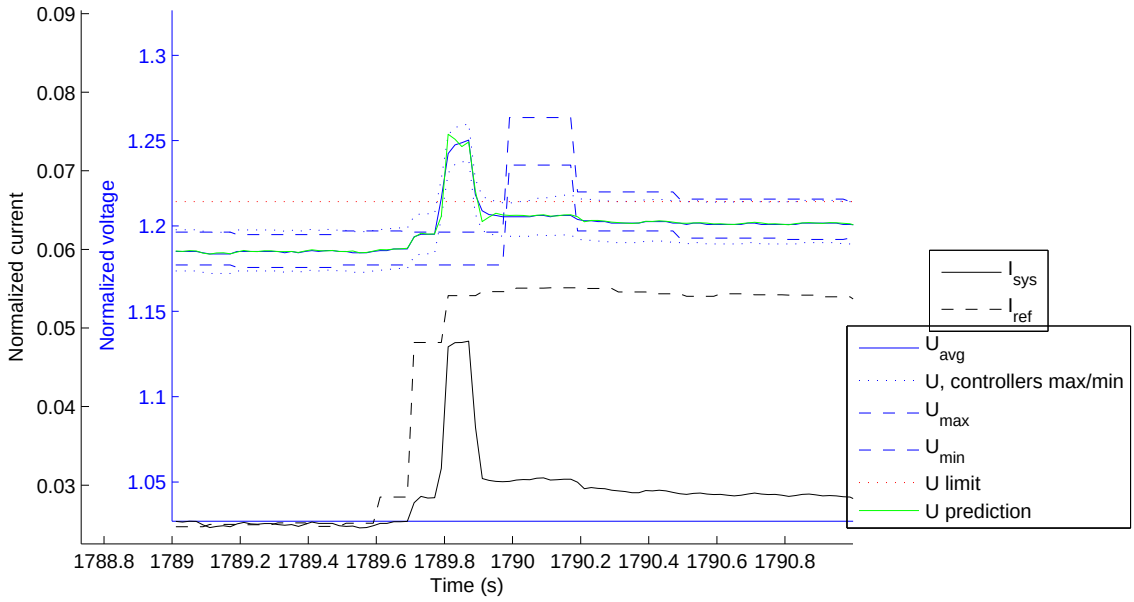

Figure 34. Current control as a result of a test with a current profile based on how the battery system could be used.

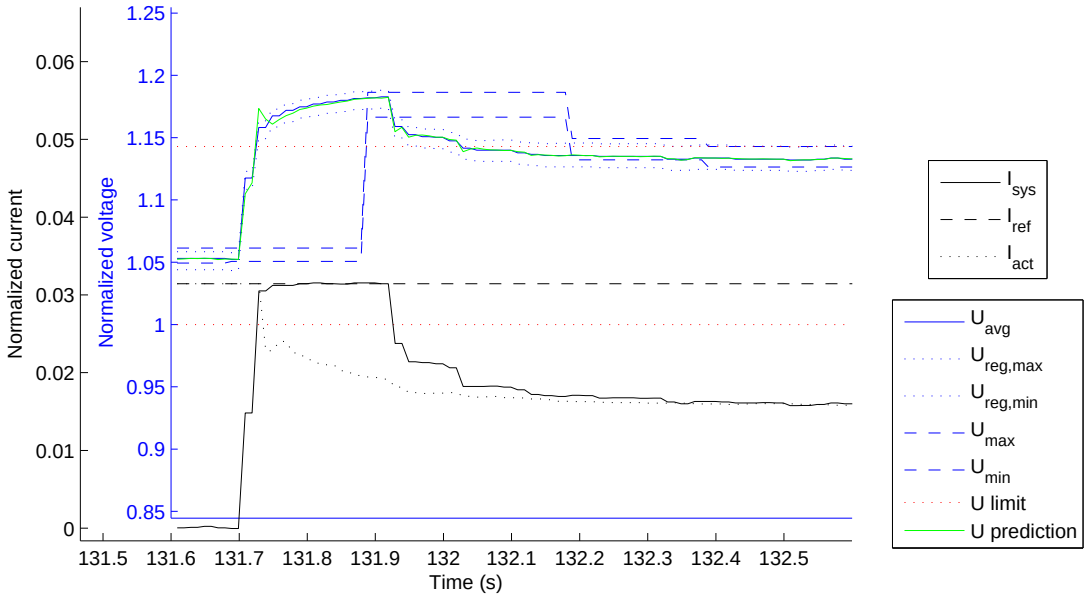

Figure 35. A step in I_{ref} with active regulation occurring during a short pulse test.

7 Conclusions

The improvement of the control performance comparing to the previously used control is generally large and during the testing within actual usage of the rig there were no unexpected behaviour even with suboptimal configurations such as an non optimal forgetting factor.

The simple approach to control a system with the cell as a pure resistance in series with a voltage source does work very well while the improvement of the higher order cell models is questionable. Additionally the adaptation is stable when considering the modelled system. But within the complete system the control performance is naturally bounded by the response of all parts, mainly the measurements that the feedback relies on and the performance of the actuator.

As the real system and testing procedures did not fulfil the stability conditions for the adaptation there are some uncertainty about the adaptive robustness. But as we see in the results there are just a small set of modifications (forgetting factor, limits on gain) that is needed to ensure that it works well in practice. If considering the stability of the control it is of highest importance to always keep the stability, and by considering the accuracy of the adapted model one can assure that there is always a large enough gain margin for the uncertainties. As the system is unknown there is an amount of uncertainty but with the security margins used in testing the results were stable as expected.

When considering performance the final control is not optimal, several possibilities exist for mitigating the different effects that are introduced in the system besides the modelled cell dynamics. Partly as a result of unmodelled dynamics, but mainly because of the uncertain properties of the measurement signals One can assume that some type of low pass filtering of the data is involved in the battery system used for testing. With the uncertainty within the treatment of data in the closed battery system, and within future battery systems, the final solution was based on just ensuring robustness.

8 Further improvements

The filtering, delay and other effects introduced by the embedded systems and the rig software could be handled in better ways. Initially one could investigate the possibilities of improving the reporting of measurements, including the possibility to use timestamps on measurements. Methods for handling packet dropout in adaptive systems also exist, as well as methods for delay compensation. Adaptation to a networked systems with unknown delays and other uncertainties may certainly be done, and improved performance could be achieved.

Bibliography

[1] Gao, Lijun; Liu, Shengyi ; Dougal, R.A, *Dynamic Lithium-Ion Battery model for System Simulation*, IEEE Transactions on Components and Packaging Technologies, Sept. 2002, Vol.25(3), pp.495-505.

[2] Gomez, Jamie ; Nelson, Ruben ; Kalu, Egwu E. ; Weatherspoon, Mark H. ; Zheng, Jim P, *Equivalent circuit model parameters of a high-power Li-ion battery: Thermal and state of charge effects*, Journal of Power Sources, 2011, Vol.196(10), pp.4826-4831

[3] Dong, T. K. Kirchev, A. ; Mattera, F. ; Kowal, J. ; Bultel, Y, *Dynamic Modeling of Li-Ion Batteries Using an Equivalent Electrical Circuit*, Journal of The Electrochemical Society, Volume 158, issue 3, pp.A326, 2011.

[4] K.H. Norian, *Equivalent circuit components of nickel–metal hydride battery at different states of charge*, Journal of Power Sources, Available online 27 April 2011.

[5] Katarina Wiezell; Nicklas Holmström; Göran Lindbergh, *Studying Low-Humidity Effects in PEFCs Using EIS*, Journal of The Electrochemical Society, volume 159, issue 8, pages F379-F392, 2012.

[6] Karl Henrik Johansson; Bo Wahlberg; Elling W. Jacobsen, *EL2620 - Nonlinear Control - Lecture notes*, Automatic Control, KTH, Stockholm, Sweden, 2011.

[7] Torkel Glad; Lennart Ljung, *Reglerteknik - Grundläggande teori*, Studentlitteratur AB, Lund, Sweden, 2011.

[8] Torkel Glad; Lennart Ljung, *Reglerteori - Flervariabla och Olinjära metoder*, Studentlitteratur AB, Lund, Sweden, 2011.

[9] K. J. Åström; B. Wittenmark, *On self tuning regulators*, Automatica, Vol. 9, pp. 185-199, 1973.

[10] Ioan Doré Landau ; Rogelio Lozano ; Mohammed M'Saad ; Alireza Karimi *Adaptive Control*, Springer London Dordrecht Heidelberg New York, 2011.

[11] James M. Krause ; Pramod P. Khergonekar, *Parameter Identification in the Presence of Non-parametric Dynamic Uncertainty*, Automatica, Vol. 26, No. 1, pp. 113-123, 1990.

[12] ISO 12405-1:2011, *Electrically propelled road vehicles – Test specification for lithium-ion traction battery packs and systems – Part 1: High power applications. Ed. 1.0*

TRITA-MAT-E 2014:13
ISRN-KTH/MAT/E—14/13-SE

www.kth.se